UNIVERSITÄTSKLINIKUM HAMBURG-EPPENDORF

Klinik und Poliklinik für Gynäkologie

Direktorin: Prof. Dr. med. Barbara Schmalfeldt

Analysis of Desmosomal Protein Desmocollin 2 and Plakophilin 1 Expression in Primary Breast Cancer and Their Roll in Metastases Development

Dissertation

zur Erlangung des Grades eines Doktors der Medizin
an der Medizinischen Fakultät der Universität Hamburg.

vorgelegt von:

Sarah Giannini Bryan
aus Carlton, Melbourne, Australien

Hamburg 2023

Angenommen von der
Medizinischen Fakultät der Universität Hamburg am 07.12.2023.

Veröffentlicht mit Genehmigung der
Medizinischen Fakultät der Universität Hamburg.

Prüfungsausschuss, die Vorsitzende: Prof. Dr. Sabine Windhorst

Prüfungsausschuss, zweite Gutachterin: Prof. Dr. Leticia Oliveira-Ferrer

Table of Contents

1 Original Publication and Supplement

RESEARCH

Open Access

The role of the desmosomal protein desmocollin 2 in tumour progression in triple negative breast cancer patients

Francesca Reimer[1†], Sarah Bryan[1†], Karen Legler[1], Thomas Karn[2], Serenella Eppenberger-Castori[3], Jakob Matschke[4], Thais Pereira-Veiga[5], Harriet Wikman[5], Isabell Witzel[1], Volkmar Müller[1], Barbara Schmalfeldt[1], Karin Milde-Langosch[1], Udo Schumacher[5,6], Christine Stürken[5,6,7†] and Leticia Oliveira-Ferrer[1*†]

Abstract

Background The disruption of epithelial features represents a critical step during breast cancer spread. In this context, the dysregulation of desmosomal proteins has been associated with malignant progression and metastasis formation. Curiously, both tumour suppressive and pro-metastatic roles have been attributed to desmosomal structures in different cancer entities. In the present study, we describe the pro-metastatic role of the desmosomal protein desmocollin 2 (DSC2) in breast cancer.

Methods We analysed the prognostic role of DSC2 at mRNA and protein level using microarray data, western blot analysis and immunohistochemistry. Functional consequences of DSC2 overexpression and DSC2 knock down were investigated in the triple negative breast cancer (TNBC) cell line MDA-MB-231 and its brain-seeking subline MDA-MB-231-BR, respectively in vitro and in vivo.

Results We found a significantly higher DSC2 expression in the more aggressive molecular subtypes HER2-positive and TNBC than in luminal breast cancers, as well as a significant correlation between increased DSC2 expression and a shorter disease-free—also in multivariate analysis—and overall survival. Additionally, a significant association between DSC2 expression in the primary tumour and an increased frequency of cerebral and lung metastasis could be observed. In vitro, ectopic DSC2 expression or DSC2 down-regulation in MDA-MB-231 and MDA-MB-231-BR led to a significant tumour cell aggregation increase and decrease, respectively. Furthermore, tumour cells displaying higher DSC2 levels showed increased chemoresistance in 3D structures, but not 2D monolayer structures, suggesting the importance of cell aggregation as a means for reduced drug diffusion. In an in vivo brain dissemination xenograft mouse model, reduced expression of DSC2 in the brain-seeking TNBC cells led to a decreased amount of circulating tumour cells/clusters and, in turn, to fewer and smaller brain metastatic lesions.

Conclusion We conclude that high DSC2 expression in primary TNBC is associated with a poorer prognosis, firstly by increasing tumour cell aggregation, secondly by reducing the diffusion and effectiveness of chemotherapeutic

†Francesca Reimer and Sarah Bryan shared first authorship

†Christine Stürken and Leticia Oliveira-Ferrer shared last authorship

*Correspondence:
Leticia Oliveira-Ferrer
ferrer@uke.de
Full list of author information is available at the end of the article

agents, and, lastly, by promoting the circulation and survival of tumour cell clusters, each of which facilitates distant organ colonisation.

Keywords DSC2, Desmosome, CTC cluster, Breast cancer, Brain metastasis, Pulmonary metastasis

Background

Breast cancer is the most common malignancy among women and the leading cause of cancer-related death in women globally, with more than 90% of mortalities associated with stage IV metastatic breast cancer [1]. Breast cancer commonly metastasises to bone marrow, lung, liver, lymph nodes and brain tissue [2]. Four molecular subtypes, namely luminal A, luminal B, HER2-positive and triple-negative breast cancer (TNBC), have been associated with different patterns of metastatic spread; bone metastases with luminal A and B subtypes, liver metastases with HER2-positive subtype, and brain and lung metastases with TNBC and HER2-positive subtypes [3–5].

Metastases develop when malignant cells lose their connection to the primary tumour (dissemination), becoming circulating tumour cells (CTCs) which can be transported in blood to distant regions of the body [6–8]. Alongside single CTCs, circulating tumour cell clusters (CTC clusters) have been detected in the blood of cancer patients [9–13]. CTC clusters, which are disseminated cell aggregates of up to 50 tumour cells, have been shown to have an up to 50-fold higher chance of forming metastases than single CTCs, and are therefore associated with worse clinical outcomes [9, 14–16]. This higher metastatic potential may be attributed to the increased resilience of CTC clusters in circulation, compared to single CTCs, which in turn increases the probability of dissemination into a distant organ [12, 17]. Further, it has been shown that CTC clusters originate as cell aggregates from the original primary tumour, rather than through intravascular aggregation or proliferation of singular CTCs [9, 18]. However, the cellular and micro-environmental factors which promote CTC cluster formation are still largely unknown.

Desmosomal proteins have been previously described to be associated with cell aggregation and, in particular, high plakoglobin expression levels have been found in CTC clusters [9, 19, 20]. Desmosomes are cell junctions which stabilise the connection between neighbouring epithelial cells. In desmosomes, the transmembrane proteins desmocollin 1–3 and desmoglein 1–4, which belong to the cadherin superfamily, form homo- and heterophilic interactions and are intracellularly connected to the intermediate filament cytoskeleton through desmosomal plaque proteins, such as plakoglobin and plakophilin (members of the armadillo family) and desmoplakin (member of the plakin family of cytolinkers) [21–23]. One theory is that an abundant expression of desmosomal proteins could lead to enhanced intercellular adhesion between disseminating tumour cells, both during CTC formation and vascular transport [9, 18, 24]. To date, studies focusing on the expression of various desmosomal proteins in a variety of primary cancer types have shown both tumour-suppressive and tumour-promoting effects on growth and metastases [9, 25–27]. Recently, the desmosomal protein desmoglein 2 (DSG2) has been associated with a poorer prognosis and higher recurrence risk in breast cancer patients. DSG2 expression is regulated by hypoxia in breast cancer cells and increases the prevalence of CTC clusters, facilitating distant metastasis [25].

This study focused specifically on desmocollin 2 (DSC2)—a transmembrane cell anchoring protein—in primary breast cancer, for which the role in breast cancer metastases formation is still not completely understood. Several studies have found that DSC2 proteins are abnormally expressed in various types of cancer and correlate with cell proliferation and invasive behaviour [28, 29], and showed that a high expression of DSC2 increased cell aggregation [20, 30]. A recently published study by Li et al. accentuates that elevated DSC2 expression, in combination with the desmosomal protein Plakophilin-1 (PKP1), can activate PI3K/AKT or CDH1 to increase cluster formation to resist shear-stress-induced cell death. Furthermore, higher expression of DSC2 and PKP1 was correlated with lower overall survival and worse disease progression in patients with breast and lung cancer [31]. The aim of this study was to investigate the potential of DSC2 at mRNA and protein level as a predisposing factor for breast cancer progression and the development of breast cancer metastases, in particular to the lung and brain.

Methods
Patient cohorts
All patients, from whom the tissue samples were derived, were treated at the University Medical Centre Hamburg-Eppendorf, Germany, Department of Gynaecology between 1991 and 2002. All patients gave written approval for the utilisation of their tissue samples and the reviewing of their medical records according to our investigational review board and ethics committee guidelines (Ethik-Kommission der Ärztekammer Hamburg,

#OB/V/03). Further cohort details and patient characteristics are listed in the Additional file 2: Table S1. Microarray analyses of DSC2 mRNA levels in patients with and without distant metastases were performed on 197 mRNA extracts from primary breast cancer tissue samples. For the western blot, a total of 111 samples were collected based on tissue availability from the same patient cohort. Slides of four tissue microarrays, constructed under permission of the Ethikkommission Beider Basel (EKBB # 395/11), kindly provided within collaborative efforts in the frame of the Pathobiology study group of the EORTC by Dr. Serenella Eppenberger-Castori from the Biobank at Institute of Medical Genetics and Pathology at the University of Basel, Switzerland, were used for immunhistochemical analysis. Patient characteristics are supplied in Additional file 3: Table S2.

Microarray data
We analysed DSC2 mRNA levels using microarray data (Affymetrix HG-U133A) from the aforementioned cohort. Here, two probe sets (204750_s_at and 204751_x_at) corresponding to DSC2 were available and analysed independently. Additionally, the mean expression value of the 2 probe sets was calculated and also included in further analyses. According to the DSC2 mRNA values of each probe set and the mean value, the cohort was divided into quartiles of similar size, representing low, moderate-low, moderate-high, and high DSC2 levels. Correlations between DSC2 mRNA levels (quartiles) and clinicopathological factors, such as histological grading, stage, lymph node involvement, oestrogen, and progesterone receptor status (ER, PR) were statistically examined by χ^2-tests. Overall survival was analysed by Kaplan–Meier analysis and log-rank tests. Additionally, the correlation between DSC2 mRNA levels (continuous data) and disease-free and overall survival was calculated using Cox regression analyses. Multivariate Cox regression analyses including the clinical stage, nodal involvement and molecular subtype were performed for all probe sets and the DSC2 mean value. Here, a backwards analysis with stepwise removal of insignificant terms was used. Probability values less than 0.05 were regarded as statistically significant. All statistical analyses were conducted using SPSS software Version 26 (SPSS Inc., Chicago, IL, USA). For validation purpose we used an independent Affymetrix microarray dataset consisting of 572 breast cancer samples from Gene Expression Omnibus (GSE2603, GSE2034, GSE12276) for which detailed information on metastatic localization was available [32].

Protein lysate preparation and western blot analysis
Tissue samples were obtained intraoperatively and immediately stored in liquid nitrogen as fresh frozen samples. The histological characteristics of each sample were evaluated on cryo-cut and haematoxylin–eosin-stained sections. The tissue was tailored, where necessary, to obtain at least 70% tumour cells in the sample used for protein extraction. Approximately 100 mg of tissue was excised and pulverised using a micro-dismembrator (Braun-Melsungen, Melsungen, Germany) for 2 min and 45 s at 200 r.p.m. Proteins were lysed in ice-cold sample buffer (50 mM Tris pH 6.8, 1% sodium dodecyl sulphate (SDS)), 10% sucrose and 10 µl/ml protease inhibitor cocktail (Sigma, Taufkirchen, Germany). For western blot analyses, volumes of tumour lysates containing 20 µg of protein were loaded per well. The following antibodies were utilised in the western blot detection process: mouse monoclonal anti-DSC2 IgG (Millipore, MABT411) dilution 1:1000, mouse monoclonal anti-β-Actin (C4) (Santa Cruz Biotechnology, sc-47778) dilution 1:2000 and goat anti-mouse IgG-HRP (Santa Cruz Biotechnology, sc-2055) dilution 1:8000. Antibodies were visualised using a chemiluminescent reagent (SuperSignal ® West Pico chemiluminescent Substrate, Thermo Scientific, Rockford, USA). Protein band intensities were quantified using a calibrated densitometer (GS-800 Imaging Densitometer, Bio-Rad, Munich, Germany). The primary breast cancer protein lysate UPA497 was used as a positive control for DSC2, with its DSC2 expression being defined as 100% for the purpose of standardisation. Protein expression values in all detected bands were also normalised using the loading control β-Actin. For the statistical analyses, these values were divided into four equal groups (quartiles), representing very low, low-moderate, moderate and high protein expression.

Breast cancer cell lines, cell culture and stable transfections
The human TNBC cell line MDA-MB231 and its brain seeking subline MDA-MB231-BR were provided by Dr Takara (University of Texas). Cells of both lines were cultivated in Dulbecco's Modified Eagle's Medium (DMEM, ThermoFisher Scientific, Waltham, MA, USA) supplemented with 10% fetal calf serum (FCS) under standard cell culture conditions. Cells were authenticated before usage. Two different DSC2-knockdown MDA-MB231-BR cell lines were generated by lentiviral transduction using vectors containing shRNA-sequences targeting specific regions of the DSC2 mRNA sequence (MISSION shRNA III and V, Sigma-Aldrich, GmbH). Similarly, a control cell line was established using a scramble shRNA sequence (Addgene, plasmid ID1864). The full DSC2 cDNA sequence obtained from a commercially available vector (Des476-Desmocollin 2-myc Plasmid; Addgene Plasmid ID: 32233) was cloned into LeGO-iC2-Puro + Plasmid (kindlykindly provided by AG Fehse, Center for Oncology, Department of Stem Cell Transplantation, UKE,

Hamburg, Germany) using BamHI and EcoRI restriction enzymes. After lentiviral production in HEK293T cells, MDA-MB231 cells were transduced. The corresponding empty vector was taken as a negative control. After selection with puromycin (2ug/mL), the level of DSC2 mRNA and protein was detected using real time quantitative polymerase chain reaction RT-PCR and western blot analysis, respectively.

RNA isolation and real-time quantitative polymerase chain reaction

RNA was isolated using the RNeasy Mini Kit (Qiagen, Hilden, Germany) and a QIAshredder (Qiagen, Hilden, Germany), and was subsequently reverse transcribed using qScriber cDNA Synthesis Kit (HighQu, Kraichtal, Germany) according to the manufacturer's instructions. RT-PCR was carried out with ORA™ qPCR Green ROX H Mix (HighQu, Kraichtal, Germany) using the StepOnePlus System (Applied Biosystems, Thermo Fisher Scientific Inc.). The data analysis was performed using the $\Delta\Delta Ct$ method. The following primers were used for DSC2: forward primer, 5'-GCCCATCTTCTTCTTGTC GTT-3'; reverse primer, 5'-CCCGTCTTGGTGAAAAAG TGT-3'. Primer sequences for the housekeeping gene were as follows: forward primer, 5'-GTCAGTGGTGGA CCTGACCT- 3'; reverse primer, 5' -TGCTGTAGCCAA ATTCGTTG-3'.

Immunofluorescence

Cells (1×10^5) were seeded on coverslips, cultured for 48 h, and fixed with 3.7% formaldehyde for 20 min at room temperature. After blocking with 1% bovine serum albumin (BSA) in phosphate buffered saline (PBS) (Mg+/Ca+) for 1 h at room temperature, cells were incubated with a polyclonal DSC2 antibody (1:50 in 1% BSA/PBS; Sigma-Aldrich, Hamburg, Germany) over night at 4 °C. Subsequent to washing, cells were incubated with a second antibody solution (mouse anti-rabbit IgG Alexa Fluor® 488; Jackson ImmunoResearch, Ely, UK; 1:500 in 1% BSA/ PBS) for 1 h at room temperature. Coverslips were carefully placed on slides using mounting medium and DAPI (Vectashield). Images were acquired using a fluorescence microscope BZ9000 and the software BZII Viewer (Keyence, Germany).

Proliferation assay

For cell proliferation analyses, the Cell Proliferation Kit II (XTT) (Roche Applied Science, Mannheim, Germany) was used according to the manufacturer's instructions. Briefly, cells were seeded in a final volume of 100 µl medium per well in a 96-well plate (1.5×10^3 MDA-MB231-BR cells per well, 2×10^3 MDA-MB231 cells per well). After 24 h, 48 h and 72 h, cell viability

was determined by adding XTT labelling mixture and by measuring the absorbance after 6 h at 490 nm using a microplate reader (DIAS Max002, Dynex Technologies, Chantilly, USA). Each experiment was performed with 12 replicates (wells) per condition ($n=12$). Images shown are representative of three independently performed experiments.

Cytotoxicity analysis

For the MDA-MB231-BR cell line and the DSC2-knock down sublines, an Annexin-V/PI staining was performed after cisplatin treatment in order to quantify the extent of apoptotic and necrotic cells. Briefly, cells were seeded into 6-well plates at a density of 2.5×10^5 cells per well, incubated for 24 h and treated with cisplatin (Accord Healthcare Limited, North Harrow, United Kingdom) in three different concentrations (10 µM, 25 µM, 50 µM) for 48 h using serum-reduced DMEM medium. Subsequently, cells within the supernatant, as well as adherent cells, which were carefully detached using AccuMax (eBioscience, San Diego, CA, USA), were stained with an APC-labelled Annexin-V antibody (Annexin-V-APC, AnxA100, MabTag GmbH, Oldenburg, Germany) for 30 min at 4 °C in the dark. After washing with PBS (+/+), cells were resuspended in 1% BSA in PBS and stained with PI (BD Pharmingen, San Diego, CA, USA). FACS analysis was performed using the FACS Calibur (BD Biosciences, Heidelberg, Germany) and all data were analysed using FlowJo Software.

DSC2 overexpressing and control MDA-MB231 cells display a strong fluorescence, due to the transduction with the previously mentioned LeGO-iC2-Puro+Plasmid, which includes the mCherry-coding sequence. For these cell lines, the cisplatin-induced cytotoxicity was assessed using XTT, as described above. Briefly, MDA-MB231 cells were seeded into 96-well plates with 2×10^4 cells in 100 µl per well. After incubating for 24 h, cells were treated with cisplatin in three different concentrations (10 µM, 25 µM, 50 µM) for 48 h and the Cell Proliferation Kit (Roche) was used as described in the previous section. Each experiment was performed in duplicates. Images shown are representative of three independently performed experiments.

Migration assay

To investigate cell migration, the Oris™ Universal Cell Migration Kit (Platypus Technologies, Madison, WI) was used according to the manufacturer's protocol. Briefly, cells were seeded (5×10^4 cells in 200 µl per well) in a 96-well plate fitted with sterile silicon stoppers using serum-reduced medium (5% FCS). After 24 h incubation, stoppers were gently removed allowing cells to migrate into the central cell-free detection zone. Migration

7

potential was assessed by analysing the cell-free area of each well at four different time points (0 h, 24 h, 48 h and 72 h post removal of stoppers) with the ImageJ Wound Healing Tool (Wayne Rasband, National Institute of Health). Each experiment was performed with 12 replicates (wells) per cell line. Images shown are representative of three independently performed experiments.

Invasion assay

Matrigel Growth Factor Reduced (BD Biosciences, Heidelberg, Germany) was diluted to a concentration of 3.5 mg/ml with serum-free medium. Afterwards, 96-well plates were coated with a 1:1 mixture of Matrigel and serum-reduced medium (5% FCS) and incubated for 30 min at 37 °C. Hereafter, Oris™ Universal Cell Migration Kit (Platypus Technologies, Madison, WI) was used according to the manufacturer's protocol as described above. After a 24 h incubation period, the stoppers and medium were carefully removed and 40 μl of newly prepared Matrigel coating solution was added. Plates were incubated again for 30 min at 37 °C. Finally, serum-reduced medium was added to all wells. For determining cell invasion potential, analyses were performed as described above. Each experiment was performed with 12 replicates (wells) per cell line. Images shown are representative of three independently performed experiments.

Cell spheroid formation

Cells were seeded at 5×10^3 cells in 200 μl medium per well on 2% agarose-coated (UltraPure™ Agarose, Invitrogen, Carlsbad, CA, USA, dissolved in PBS) 96-well plates. To assess and observe spheroid formation of cells, spheroids were examined and documented every second day using light microscopy and a camera (Axiovert 40 C, Carl Zeiss AG, Leica DFC320, Wetzlar, Germany). For further investigation of compactness, spheroids were dissociated by pipetting each spheroid up and down five times and by comparing formation immediately afterwards. Each cell line was seeded in quadruplicates. Images shown are representative of three independently performed experiments.

Cytotoxicity in a 3D Model

Cisplatin-induced cell cytotoxicity on 3D-structures was assessed using immunocytochemical detection of phosphorylated gamma H2AX (γH2AX)—an established marker for DNA double-strand breaks—on tumour cell aggregates grown on polyHEMA (Sigma-Aldrich) coated flasks. Here, cell lines were seeded at a density of 2×10^6 cells in 12 ml per polyHEMA coated T75 culture flask and cultured as cell aggregates for 72 h. Subsequently, cells were incubated with cisplatin in a final concentration of 50 μM for 8 h and 24 h, and were subsequently fixed in formalin, embedded into 2% agar (Agar NOBEL, Difco Laboratories, Detroit, MI, USA) and then embedded in paraffin. Slides from FFPE-cells were pre-treated in a steamer (citrate buffer pH 6.0) at 125 °C for 4 min and S1699 (pH 6.0, DAKO) at 121° C for 10 min, respectively) and incubated with an anti-DSC2 (1:25 HPA011911, Atlas Antibodies, Sigma-Aldrich, Hamburg, Germany) or an anti-γH2A.X antibody (1:10,000; ab81299, abcam, Berlin, Germany) for 1 h at room temperature. Incubation with biotin-labelled swine anti-rabbit secondary antibody occurred for 30 min at room temperature (1:200 dilution in TBS, E0353, DAKO, Glostrup, Denmark). For detection, sections were incubated with Vectastain® ABC-AP Kit (Vector Laboratories, Burlingame, CA USA) for 30 min and stained with Permanent Red (K0640, DAKO, Glostrup, Denmark). Rabbit immunoglobulin normal fraction (X0903, Agilent, Santa Clara, CA, USA) was used as a negative control for the anti-γH2A.x primary antibody. A rabbit polyclonal IgG (ab37415, abcam, Berlin, Germany) was used as a negative control for anti-DSC2 primary antibody. All slides were slightly counterstained with haematoxylin. Stained slides were scanned using the Axio Scan.Z1 (Zeiss, Jena, Germany) and images were acquired using netScope Viewer Pro software version 1.0.7079.25167 (NetBase Software GmbH, Freiburg, Germany). For quantifying the γH2A.X staining, manual counts of positive stained cells (4×100 cells in 4 different areas of each slide) were performed using the assistant electronic memory counter Counter AC-15 (Karl Hecht Assistant, Altnau; Switzerland).

Intracardiac metastasis mouse model

The intracardiac mouse model was conducted as previously described [33]. Briefly, female 8 to 9-week-old SCID mice (CB17/lcr-Prkdcscid/lcrlcoCrl) were anesthetized and 1×10^6 tumour cells were injected intracardially into the left ventricle of the heart (n = 15 per group). Tumour cells were previously transduced with luciferase-bearing plasmid and bioluminescence signals were tested before injection via bioluminescence imaging (BLI). After intracardiac injection, tumour cell dissemination was monitored weekly under BLI. Assessment of subsequent metastases was monitored in vivo weekly by imaging for up to 3 weeks. Mice showing termination criteria were immediately sacrificed. At the endpoint (21 days), animals were anesthetized and blood was collected from the left ventricle by cardiac puncture immediately before the final killing was executed by cervical dislocation. Ex vivo bioluminescence imaging was conducted from the lungs and brain. Lungs and brain were equally divided and frozen down for DNA isolation and subsequent ALU-PCR or paraffin-embedded for further analysis (H&E and luciferin staining) as previously described [33, 34]. The

animal experiments were approved by the Authority for Social Affairs, Family, Health, and Consumer Protection of the Free and Hanseatic City of Hamburg through application N005/2020.

Histology and immunohistochemistry

The whole brain and the right lung of the mice were fixed in 4% buffered formalin and processed for wax histology. 4 µm sections were cut from brain for immunohistochemistry and 10 sections from the middle of the block were stained with hematoxylin and eosin (H.E.). The lungs were fixed en block and subsequently cut into 1 mm thick slices and embedded in 2% agar. Afterwards, the lung slices were paraffin-embedded and cut into 4 µm thick sections. Ten sections of each paraffin wax block were H.E. stained and metastases were counted at a 200-fold magnification using Zeiss Axiophot photomicroscope (Zeiss, Jena, Germany). Additionally, two series of serial sections out of the middle of each paraffin wax block were preserved for further immunohistochemical analyses. The immunohistochemical staining was performed on 4 µm sections. Sections were deparaffinized in descending ethanol concentrations and pre-treated with citrate buffer solution (pH 6.1) in a steamer for 4 min. After incubation for 1 h at room temperature with the primary antibody DSC2 (Atlas, HPA011911), samples were washed twice with TBS-T (TBS + 0.1% TWEEN-20) and once with TBS for 5 min. After incubation with anti-rabbit secondary antibody (LS-Bio, LS-C350860) for 30 min at room temperature, antibody binding was visualized using the Vectastain ABC-AP Kit (VectorLabs., Burlingame, CA, USA) and Permanent Red Solution (Dako) according to the manufacturer's instruction. The nuclei were counterstained in Mayer's hemalum solution.

Circulating tumour cell detection

Mouse blood samples (200–500 µl) were obtained via cardiac puncture and collected into EDTA KE/1.3 tubes (Sarstedt, Germany). To perform cardiac puncture, mice were deeply anaesthetized under isoflurane, and a 21-gauge needle coated with heparin was inserted into the heart. Mice were euthanized immediately following the cardiac puncture. Blood samples were processed on the label-independent, microfluidic system Parsortix® (ANGLE plc., United Kingdom), a device designed for the size-based capture of rare cells from whole blood [35]. The isolated cells were harvested and spun onto a glass slide (190 g, 7 min). Slides were dried overnight at room temperature and stored at − 80 °C until further analysis.

Tumour cells isolated with the Parsortix® system were identified via immunocytochemistry. Briefly, dried cytospin slides were brought to room temperature and fixed with 2% PFA (Sigma Aldrich, Germany) for 10 min. The

samples were washed with 0.5 mL of 1x-PBS prior to permeabilization with 0.1% Triton X 100/PBS (Sigma Aldrich, Germany) for 10 min. Following two additional wash steps, 10% AB-serum/PBS (BioRad, Germany) was applied for blocking (60 min). Standard detection of CTCs is usually achieved with epithelial antibodies [36], however, TNBC cells lack epithelial markers and are successfully detected with CD298 [37]. Subsequently, directly anti-human PE labelled CD298 (clone LNH-94, Biolegend, USA) and anti-mouse Alexa Fluor 488 conjugated CD45 (clone HI30, Biolegend, USA) antibodies were incubated for 60 min, followed by 5 min of DAPI-incubation (1 µg/mL). Cytospins were covered with Prolong Gold Antifade Reagent (Thermo Fisher Scientific, Dreieich, Germany), sealed with a cover slip and examined by fluorescence microscopy (Axio Observer 7, Zeiss). CD298-positive, DAPI-positive, CD45-negative cells with intact morphology were defined as tumour cells. Clusters were defined when 2 or more cells were found together.

Statistical analyses

All statistical analyses were performed using SPSS Statistics version 24 for Windows (IBM, Armonk, NY, USA). Correlations between mRNA and protein expression values were assessed using two-sided Pearson tests. Chi-square tests were used to correlate both mRNA expression (Microarray data, cohort A) and protein expression (WB data, cohort B) with the following clinical and pathological parameters; histological grading (G1/G2/G3), molecular subtype (Luminal/HER2 positive/TNBC), ER and PR Status (positive/negative) and the presence of metastases (loco-regional/bone/lung/visceral/brain). Kaplan–Meier estimates and the log-rank test were carried out to ascertain and compare disease-free and overall survival. The associated hazard ratios for the multivariate analyses were determined by Cox regression. Proliferation assays and cytotoxicity assays measured with XTT were statistically analysed using GraphPad Prism 5 (GraphPad, La Jolla, CA, USA). Each in vitro assay was performed at least three times. Statistical significance was assessed using unpaired two-tailed Student's t-test. The assumption of homogeneity of variances was checked via Levene's Test of Equality of Variances ($p > 0.05$). Results are given as mean ± s.d. or s.e. Probability values (p-value) ≤ 0.05 were considered to be statistically significant.

Results

High DSC2 mRNA levels are associated with the triple negative breast cancer subtype, an increased brain and lung metastasis risk and a decreased disease-free and overall survival for breast cancer patients

DSC2 mRNA levels were evaluated in 197 tumour samples of breast cancer patients using microarray data

from our own cohort (see description in material and methods). Two different probe sets (204750_s_at and 204751_x_at) corresponding to DSC2, as well as the mean value of these two probe sets, were analysed. For each probe set and the mean value, the cohort was firstly divided into quartiles (Q) according to DSC2 expression: low (Q1), moderate-low (Q2), moderate-high (Q3), and high (Q4). Correlations between DSC2 mRNA levels and clinicopathological factors such as histological grading, stage, lymph node involvement, oestrogen and progesterone receptor status (ER, PR) and molecular subtype, showed a significant association between high DSC2 levels (Q4) and higher tumour grading (in one probe set), ER- (in one probe set and the mean value), PR-negativity (in one probe set) and molecular subtype (in two probe sets and the mean value), whereas no correlation between DSC2 and tumour stage or nodal status was found. Further, high DSC2 mRNA levels significantly correlated with the development of cerebral metastases (in one probe set and the mean value). Survival analyses showed a significant correlation between high DSC2 values and a shorter overall survival (in both probe sets and mean value) and disease-free survival (in both probe sets and the mean value). All mentioned statistical correlations using DSC2 quartiles or continuous values are listed in the Additional file 4: Table S3, including the corresponding p-values.

For the DSC2 mean values, further analyses were carried out and are represented in Fig. 1. Here, HER2-positive and TNBC, which represent the most aggressive molecular subtypes, display higher DSC2 mRNA levels in comparison to the luminal subtype (p < 0.005; Fig. 1A). Also, primary tumours from patients that developed brain metastases showed higher DSC2 levels than those with no cerebral metastases (p = 0.012; Fig. 1B). Kaplan Meier analysis showed a significant association between high DSC2 levels and shorter overall survival using quartiles (p = 0.035; Fig. 1C) and a clear trend in the correlation between DSC2 and disease-free interval (p = 0.051; Fig. 1C). When we grouped patients included in quartiles Q1 to Q3 and compare them with patients with high DSC2 level (Q4) the differences in overall and disease-free survival became stronger (p = 0.004 and p = 0.015, respectively; Fig. 1C). In multivariate Cox regression analyses, including clinical stage, nodal involvement, and molecular subtype, DSC2 remained a prognostic indicator for disease-free survival (p = 0.008; HR 2.071; 95% CI 1207–3553, Additional file 4: Table S3). Interestingly, in a stratified survival analysis using this cut-off (cut-off-Q4), we found that the impact of DSC2 on overall survival (not shown) and disease-free survival was limited to the group of TNBC and HER2-positive patients (p = 0.0016 and p = 0.004, respectively; Fig. 1D), whereas in patients with luminal breast cancer the DSC2 level did not influence the survival time.
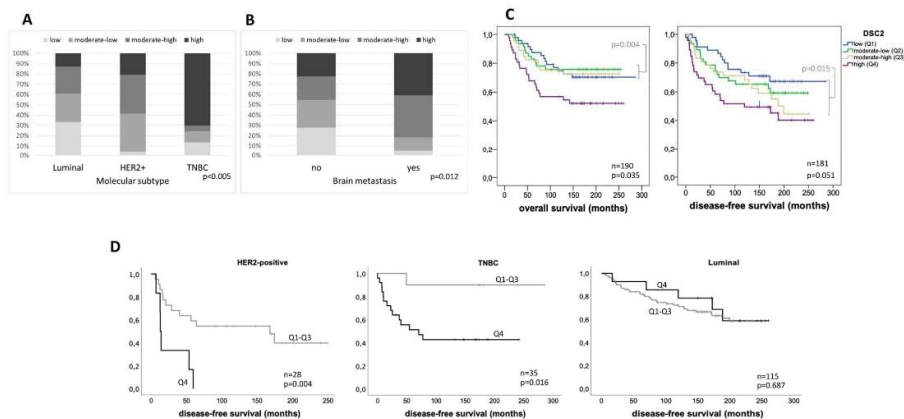

Fig. 1 Quantitative expression of DSC2 mRNA in primary breast cancer tissue and its correlation with clinicopathological variables. **A** The TNBC molecular subtype is significantly associated with high DSC2 expression (p < 0.005). **B** A highly significant association between the development of cerebral metastases and high DSC2 expression was observed (p = 0.012). **C** Both, the disease-free survival (p = 0.051; right) and the overall survival (p = 0.035; left) are reduced in patients whose tumours express high levels of DSC2. **D** Stratification analysis showed a significant association between high DSC2 levels and shorter disease-free survival only in patients with HER2-positive and TNBC

The impact of DSC2 on disease-free survival could be corroborated in a second cohort including 572 breast cancer samples (see description in material and methods and Additional file 1: Fig. S1). Here, we found a significant correlation of DSC2 mRNA expression with molecular subtype (p < 0.001; Additional file 1: Fig. S1A), brain and lung metastasis formation (p = 0.003 and p < 0.001, respectively; Additional file 1: Fig. S1B, C), as well as with disease-free survival (p < 0.001; Additional file 1: Fig. S1D) and, specifically, brain metastasis-relapse free survival (p < 0.001; Additional file 1: Fig. S1E).

Western blot analyses detected a wide variance in DSC2 expression in primary breast cancers and a significant association with DSC2 mRNA levels

Of the 197 tumour samples tested in the microarray analyses, 111 were further analysed at a protein level using western blot. Patient characteristics were similar in both groups (Additional file 2: Table S1). The western blot

results showed a wide range of DSC2 expression, varying between very low and very high expression. Additional to the expected band at 110 kDa, as described in the biological information provided by the antibody manufacturer, one or more additional bands were detected by the anti-DSC2 antibody in most samples (Fig. 2A). These bands presented, for the majority of the samples, as two double band sets between 60 and 85 kDa, and 93 and 110 kDa respectively. All samples were (at least lightly) positive for at least one of these double band sets. Since the origin and nature of these additional bands was not clear, both double band sets (individually and combined), as well as the single DSC2 band at 110 kDa (as specified by the manufacturer) were quantified by densitometry. The single band at 110 kDa and the double band between 93 and 110 kDa correlate with a coefficient of r = 0.936, while all bands combined (both double band sets) show a correlation of r = 0.676 (both p < 0.0000; Additional file 5: Table S4). In addition, all bands showed a moderate and
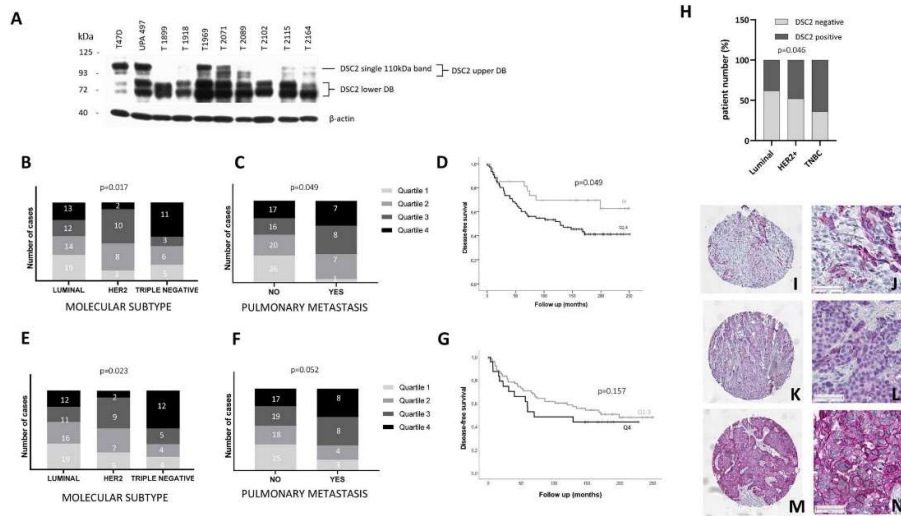

Fig. 2 Quantitative expression of DSC2 in primary breast cancer protein lysates and its correlation with clinicopathological variables. **A** Western blots depicting representative expression of DSC2 in a variety of primary breast cancer samples. Protein lysates from the breast cancer cell line T47D, as well as the breast cancer lysate UPA 497, were used as positive controls for DSC2. β-actin protein expression was quantified as a loading control. Tumours with high DSC2 levels are significantly associated with the TNBC molecular subtype (**B** all WB DSC2 bands; p = 0.017 and **E** upper WB DSC2 band; p = 0.023). A significant association was observed between high DSC2 expression and the development of pulmonary metastases (**C** all WB DSC2 bands; p = 0.049 and **F** upper band; p = 0.052). Disease-free survival in accordance with DSC2 expression levels: Patients with a moderate to high DSC2 expression level have a significantly shorter disease-free survival, compared with patients whose tumours possess no or little DSC2 (**D** all WB DSC2 bands; p = 0.049 and **G** upper WB DSC2 band; p = 0.157). **H** Immunohistochemical analysis of primary breast cancer tissue confirmed a significant association between high DSC2 levels and TNBC subtype (p = 0.046). Representative DSC2 staining results from luminal (**I–J**), HER2 positive (**K**, **L**) and TNBC (**M**, **N**)

11

significant correlation with DSC2 mRNA expression as obtained via microarray analyses (Pearson correlation coefficient $r > 0.4$; $p < 0.001$; Additional file 5: Table S4). These results suggest that all bands are isoforms and/or a result of different posttranslational modification, i.e. glycosylation. In the following analyses, we confine ourselves to the collective assessment of all detected DSC2 bands, as well as to the upper band, although similar results were obtained from analyses of each individual band, as well as each double band set.

The significant trend between molecular subtype and DSC2 expression seen at mRNA level could also be demonstrated at a protein level. While high DSC2 levels were significantly associated with the TNBC subtype, moderate and low DSC2 levels were more often observed in the HER2 and luminal subtypes respectively ($p = 0.017$ and $p = 0.023$; Fig. 2B and E). This association was further substantiated by the findings that tumours lacking PR- and ER- expression were likewise individually significantly associated with high DSC2 levels (all bands: $p = 0.046$ and $p = 0.04$ and upper band: $p = 0.054$ and $p = 0.012$ respectively; Additional file 1: Fig. S2). High DSC2 expression was, at the protein level, significantly associated with an increased risk of pulmonary metastases (all bands: $p = 0.049$ and upper band: $p = 0.052$; Fig. 2C and F). There was no significant association between high levels of DSC2 and increased risk of developing cerebral metastases in our cohort, although a trend towards this effect was observed (all bands: $p = 0.405$, upper band: $p = 0.42$). Patients whose tumours possessed increased levels of DSC2 sustained a shorter disease-free survival period in comparison to patients with low DSC2 expression (all bands: $p = 0.049$ and upper band: $p = 0.157$ Fig. 2D and G). No significant trend was observed between the patients' overall survival and the level of DSC2 expressed in their tumour.

Immunohistochemical verification of DSC2 expression in primary breast cancer samples

To further validate our findings at the protein level, DSC2 immunohistochemical staining was carried out on primary breast cancer samples included in four different tissue microarrays (TMAs). From the original 340 punctures included in the TMAs, only 243 could be evaluated. The remaining, non-analysable punctures were missing, lacking tumour cells or necrotic. Further, only primary breast cancer tissue was included in our analyses ($n = 226$), adjacent healthy tissue or metastatic tissue was excluded. DSC2 expression was observed exclusively in tumour cells in all biopsies. In positively stained tumour cells, we observed mainly a membranous staining, although DSC2 could be also detected in a minority of samples within the cytosol. Patient survival data was

only available for a small group of samples and therefore corresponding correlation analyses were not performed. Information regarding the molecular subtype was available for 175 tissue samples. Here, we evaluated 21 luminal, 77 HER2 positive and 77 TNBC tissue samples. A positive DSC2 staining was detectable in 38% of the luminal, in 48% of HER2 positive and 64% of TNBC biopsies (Fig. 2H). While all positive stained luminal samples showed a moderate staining ($2 < IRS < 6$), approx. 20% of HER2 positive and TNBC tumours displayed a strong DSC2 staining ($IRS > 6$). Figure 2 shows representative DSC2 staining results from luminal (Fig. 2I, J), HER2 positive (Fig. 2K, L) and TNBC (Fig. 2M–L).

Generation of DSC2-knockdown and overexpression in triple negative breast cancer cell lines

To assess the impact of DSC2 in breast cancer cells, we performed DSC2 knockdown in MDA-MB231-BR cells, which endogenously express a higher level of DSC2 than the parental cell line MDA-MB231. Among all sublines generated by transfection with 5 different DSC2-specific shRNAs sequences, shRNA III and V—which showed around 70% and 60% DSC2-knockdown at mRNA level (Fig. 3A) respectively, compared to the scramble control—were chosen for further analysis. A clear reduction in the DSC2 expression level in these cells could be corroborated by western blot (Fig. 3B). In addition, we chose the parental cell line MDA-MB231 for DSC2 overexpression. Here, stable lentiviral transduction with the LeGO-iC2 DSC2 vector induced a strong DSC2 overexpression in comparison with the empty vector-transduced cells, as detected by qRT-PCR and western blot (Fig. 3B). Here, the membranous localisation of DSC2 was further corroborated using immunofluorescence and flow cytometry (Fig. 3C and D, respectively).

Influence of DSC2 expression on the proliferation, migration, invasion and chemosensitivity of breast cancer cells in a 2D cell culture

The impact of reduced or increased DSC2 expression on diverse cellular properties of the TNBC cells was analysed in 2D cell culture conditions using the stably transfected MDA-MB231-BR and MDA-MB231 cells as previously described. We observed no significant differences in cell proliferation between MDA-MB231 control cells and those with increased DSC2 expression (LeGO-iC2 DSC2; Fig. 4A, upper panel). A significant increase in proliferation was only observed between MDA-MB231-BR scramble control cells and those with reduced DSC2 expression (only in shRNA III cells) after 72 h. As this result was observed only in 1 of 3 experiments (Fig. 4a, lower panel), we conclude that a DSC2 down-regulation does not affect cell proliferation in the brain-seeking cell
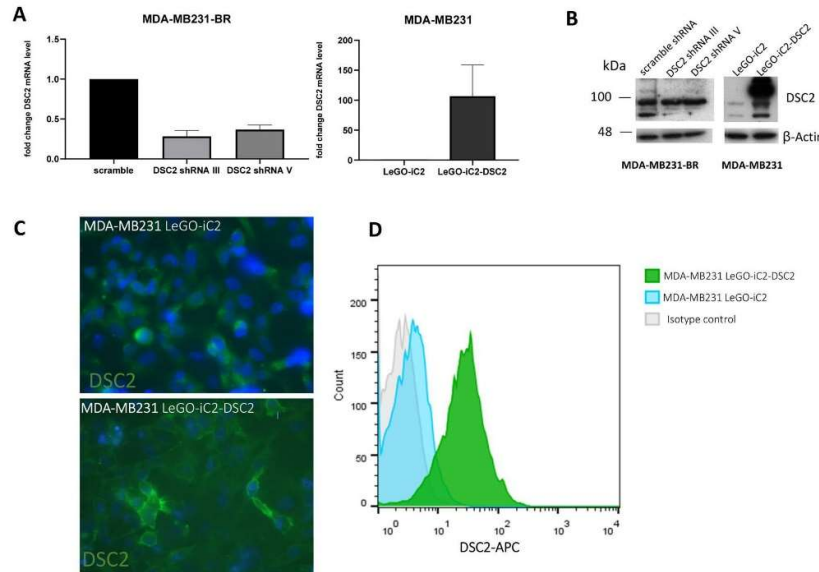
Fig. 3 Desmocollin 2 knock down and overexpression in TNBC cell lines. DSC2 knock down in MDA-MB-231-BR cells and DSC2 overexpression in MDA-MB-231 cells were performed and validated at mRNA level via qRT-PCR (**A**) and protein level using Western Blot (**B**). Additionally, membranous DSC2 expression was visualized and quantified by immunofluorescence (**C**) and flow cytometry (**D**)

line. In wound healing assays with silicon stoppers, DSC2 knock down in the shRNA III clone led to a significant (yet slight) increase in cell migration and therefore to an accelerated wound closure, whereas the shRNA V clone resembled the scramble control. Accordingly, DSC2 overexpression decreased cell migration and therefore slowed wound closure, however the difference is again too small to be conclusive (Fig. 4B).

Furthermore, when comparing MDA-MB231-BR cells with reduced DSC2 expression to MDA-MB231-BR control cells, no significant differences in the amount of apoptotic and necrotic cells, measured by flow cytometry and Annexin V and PI staining, respectively, could be noted after exposure to the cytostatic drug cisplatin for 48 h. The chemosensitivity of MDA-MB231 cells was also not affected after DSC2 overexpression, as measured using an XTT-assay (Fig. 4C).

Impact of DSC2 expression on breast cancer cell aggregation and chemosensitivity in a 3D cell culture
We next analysed the impact of DSC2 overexpression and DSC2 knock down on the cellular properties of the two TNBC cell lines in a 3D model. We observed clear

differences in the aggregation capacity between the different sublines, as shown in Fig. 5A. Here, MDA-MB231-BR cells with reduced DSC2 expression (shRNA III) failed to build compact spheroids in comparison to the corresponding control cells (scramble shRNA), when seeded on agarose coated surfaces. The differences in the aggregation capacity and compactness were even more clear after mechanical disaggregation by slowly pipetting, showing full disaggregation mostly to single cells and small cell aggregates of only a few cells in the DSC2 knock down cells, whereas the control cells remained as small cell aggregates that were able to adhere to each other again over time. Contrary to our expectations, MDA-MB231 cells with enhanced DSC2 expression did not show any phenotypical differences in the spheroid formation assay in comparison to the corresponding empty vector control cells. However, we observed a clearly enhanced compactness—which could be confirmed after mechanical disaggregation—when compared with the wild type parental cell line (WT). Quantification of the DSC2 mRNA level in the parental cell line revealed a DSC2 up-regulation (f.c. 2.3; Additional file 1: Fig. S3) in the control cell line (LeG-iC2) compared with
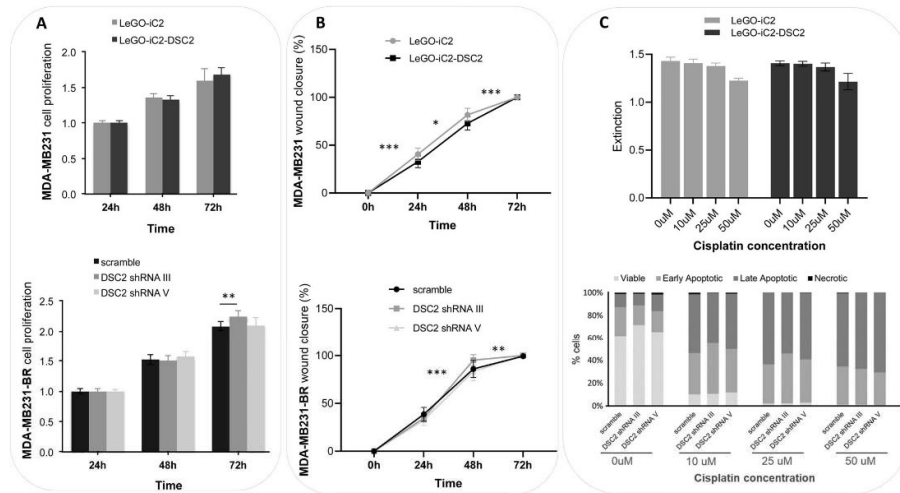
Fig. 4 Impact of DSC2 knock down and DSC2 overexpression on tumour cell proliferation, migration and chemosensitivity in 2D. **A** DSC2 overexpression in MDA-MB231 cells does not affect cell proliferation (upper panel). A slight increase in the proliferation rate was detected in one of the DSC2 knock out clones and only after 72 h cultivation (lower panel). **B** DSC2 overexpression in MDA-MB231 and DSC2 silencing in MDA-MB231-BR cells slightly but significantly decreased (upper panel) and increased (lower panel) the tumour cell migratory ability in a wound closure assay, respectively. **C** Both DSC2 overexpression (upper panel) and silencing (lower panel) did not show any impact on tumour cell chemosensitivity against cisplatin

WT cells. This unspecific and treatment-induced DSC2 deregulation in the MDA-MB231 LeGO-iC2 cells might explain the unexpectedly similar behaviour of the two sublines in the 3D model.

In order to study whether the mechanical stiffness of the cellular aggregates further influences drug diffusion and, in turn, chemosensitivity, we cultured cells of the aforementioned cell lines with different DSC2 expression levels on polyHEMA coated culture flasks, allowing them to form cell aggregates in suspension, and treated them subsequently with cisplatin for 8 and 24 h. The differences in spheroid shape observed in the aforementioned agarose model were also observed under polyHEMA culture conditions. Quantification of cisplatin-mediated DNA intra-strand cross-links (Additional file 1: Fig. S4 & materials and methods) and cisplatin-induced cell cytotoxicity on 3D cellular structures were assessed using immunocytochemical detection of PT-GG adducts and phosphorylated gamma H2AX (γH2AX)—an established marker for DNA double-strand breaks-, respectively. Here, we observed a significant increase in the number of platin adducts and DNA damaged cells in the MDA-MB231-BR subline with reduced DSC2 expression (shRNA III) compared with the control cells (scramble).

Correspondingly, we observed a significantly reduced number of platin adducts and γH2AX positive cells in the MDA-MB231 cell line with DSC2 overexpression, when compared with the WT (Fig. 5B).

Reduced DSC2 expression in MDA-MB-231-BR cells decreases metastatic potential in vivo

Next, the role of DSC2 in TNBC cells during metastasis development was analysed in vivo. Here, using the brain-seeking cell line MDA-MB-231-BR, the corresponding scramble and DSC2 shRNA cells (shRNA III) were injected (1×10^6 cells each) intracardially into the left ventricle of 8–9 weeks old female SCID mice. Although 15 mice per group were injected initially, 12 mice showed poor physical condition or strong bioluminescence signals in the lungs and thus needed to be removed at the beginning of the experiment. Therefore, 9 mice in the control group and 10 mice in the DSC2 shRNA group were further monitored weekly by BLI. One mouse from the control group and two from the DSC2 shRNA group showing hind limb paralysis were sacrificed on day 18. The remaining mice were sacrificed 21 days after cancer cell injection. Figure 6A shows representative bioluminescence images of three mice and their corresponding
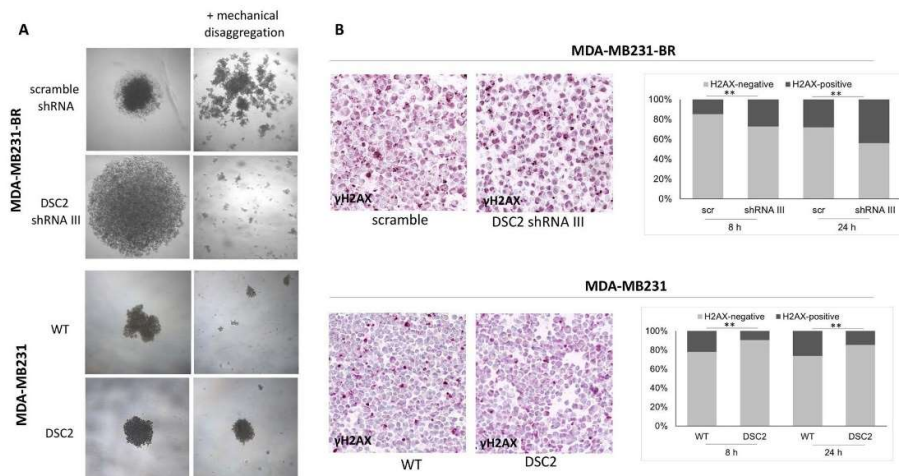
14

Fig. 5 Impact of DSC2 knock down and DSC2 overexpression on tumour cell aggregation and chemosensitivity in 3D. **A** DSC2 knock down in MDA-MB231-BR cells led to an impaired tumour cell aggregation in a 3D spheroid formation assay (upper panel), whereas DSC2 overexpression increased the compactness of the spheroids in comparison to WT, which could not be dissociated by mechanical disaggregation. **B** DNA double-strand breaks were quantified in MDA-MB231-BR DSC2 knock down cell vs. control (upper panel) and in MDA-MB231 DSC2 overexpressing cells vs. WT growing in 3D (polyHEMA) after cisplatin treatment using immunocytochemical detection of phosphorylated H2AX (γH2AX). The quantification of the aforementioned staining revealed a significant increase of cisplatin-induced cell cytotoxicity in DSC2 knock down cells (upper panel) and a significant reduced amount of DNA double-strand breaks in DSC2 overexpressing cells (lower panel)

ex vivo brains from each test group 21 days after injection. The overall tumour burden in both mice groups did not strongly differ, while ex vivo bioluminescence signals in the scramble vs. DSC2 shRNA group (mean values: brain $= 2,2 \times 10^8$ vs. $3,6 \times 10^7$ and lung $= 1,5 \times 10^8$ vs. $3,4 \times 10^7$ photons/sec), as well as the amount of disseminated tumour cells (DTCs) in the brain and lung by ALU-PCR (mean values: brain $= 76,5$ vs. 48,3 and lung $= 61,6$ vs. 23,9 DTCs/60 ng DNA) clearly showed a reduced metastatic load in the DSC2 shRNA group (Fig. 6A and D). In line with this finding, we found a reduced number of circulating tumour cells (CTCs) and circulating tumour cell clusters in the blood samples from mice corresponding to the DSC2 knock down group compared to the control group (Fig. 6C). The histological analysis of the brains and the tumour cell visualization using a specific luciferase staining (Fig. 6D) showed indeed smaller metastatic lesions in DSC2 knock down mice, consisting mostly of single cells or small cell aggregates, whereas larger metastases were found in the brains of the control mice group. The presence of microscopically detectable lung metastases was also confirmed upon histological examination of the right lung. In the DSC2 knock down mice, we detected more intravascular metastases than established pulmonary metastatic lesions, when compared to the control group (Fig. 6D).

Discussion

Desmosomes are important structures for intercellular adhesion and are functionally present most abundantly in tissue exposed to high levels of mechanical stress, such as the epidermis and myocardium [38]. In recent years, desmosomal proteins have become a point of interest in cancer research. Depending on protein type and primary tumour localisation, both tumour-enhancing and tumour-suppressive effects of desmosomal protein up/down-regulation have been observed [39]. Desmoglein 2, desmocollin 2 (DSC2) and plakophilin 1 (PKP1) have been recently linked to an increased metastatic potential of breast cancer cells by promoting cell clustering and enhanced survival during the tumour cell dissemination process [25, 31]. In the present study, we have analysed the role of DSC2 as a prognostic and predictive factor for primary breast cancer and the development of breast cancer metastases. In order to address this question, DSC2 levels at mRNA and protein levels were correlated with clinical and histopathological data. Our research has been able to show, for the first time, that higher levels of
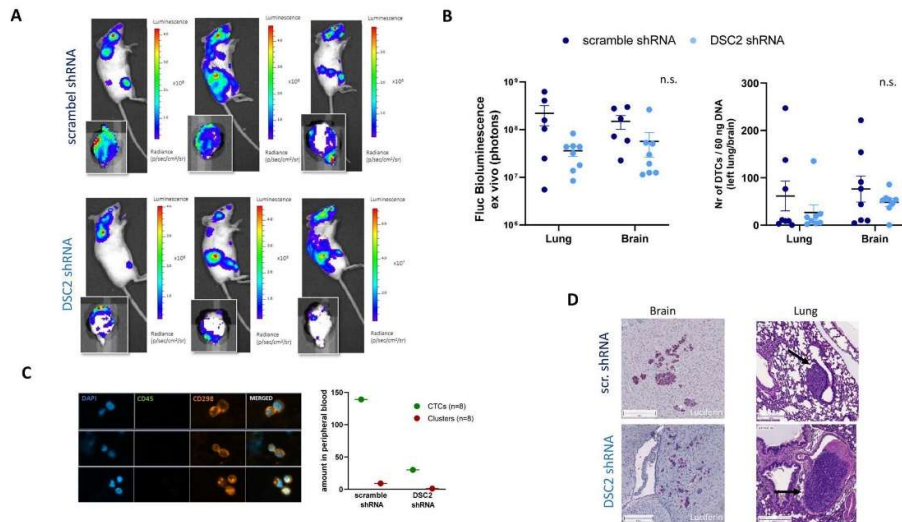
15

Fig. 6 Role of DSC2 on TNBC cell dissemination in an intracardiac mouse model in vivo. **A** Representative BLI pictures of whole mice and the corresponding ex vivo brain of each group (MDA-MB231-BR DSC2 shRNA and MDA-MB231-BR scramble shRNA) 21 days after injection. **B** The quantification of ex vivo BLI signals (*left panel*) and amount of disseminated tumour cells (ALU-PCR; *right panel*) from brains and lungs revealed a lower metastatic load in organs from mice bearing DSC2 knock down tumours in comparison with those injected with the control cell line. **C** Reduced levels of CTCs and CTCCs (circulating tumour cell clusters) were quantified in the DSC2 knock down group (n = 8, blood was pooled for analysis) in comparison to the control group (n = 8, blood was pooled for analysis). Representative pictures of CTCCs isolated from the DSC2 knock down group showing CD298 positivity and a CD45 negative staining. **D** Small metastatic lesions in the brain and lungs were detected by specific luciferase staining. In the brain of DSC2 knock down mice mainly single cells or small cell aggregates were detected, whereas larger metastases were found in the brains of the control scramble mice group. Microscopically detectable intravasal lung metastases in a DSC2 knock down mice and established metastatic lesion in a control mouse. Black file marks metastatic tumour cells

DSC2 in primary breast cancer tissue significantly influence disease progression and metastatic behaviour in HER2 positive and TNBC patients. Functionally, the extent of DSC2 expression in tumour cells directly impacts their capacity to aggregate and, in turn, influences their chemosensitivity, as shown in in vitro analyses after DSC2 up-regulation and DSC2 silencing in the TNBC cell line MDA-MB-231 and its brain-seeking subline MDA-MB-231-BR, respectively. In vivo DSC2 knock down reduces the amount of circulating tumour cells and clusters, and consequently the amount and size of established brain metastases and established metastatic lesions in lung tissue.

As mentioned, desmosomal proteins and specifically DSC2 have been previously investigated in the context of cancer research. For example, in colorectal cancer, DSC2 loss enhances tumour cell growth by altering the Akt/β-catenin signal pathway [29]. Furthermore, knock-down of desmosomal proteins such as DSC2, DSG2 and plakoglobin was reported to impair cell aggregation and reduce anoikis resistance in lung and breast cancer cells, while their expression levels were correlated with poor overall survival in lung cancer patients and poor metastasis-free survival in breast cancer patients [19]. A similar effect of DSC2 and DSG2 mediated cell adhesion on cell aggregation was detected in colon cancer spheroids [20]. Aceto et al. detected an up-regulation of plakoglobin and other desmosomal components in CTC clusters of breast cancer patients and revealed its importance for the formation of CTC clusters and distant metastases [9]. And, in a more recent study, breast and lung cancer cells resistant to shear stress revealed an up-regulation of DSC2 and PKP1, leading to more CTC cluster formation and enhanced cell survival in circulation via activation of the PI3K/AKT/Bcl-2 pathway [31]. Here, our findings suggest that the aforementioned DSC2 mediated effect on tumour cell aggregation and survival applies for TNBC as well.

In the present study, we found that tumour DSC2 levels significantly influence the disease-free and

16

overall survival of breast cancer patients, in particular for patients with primary tumours corresponding to the HER2 positive and TNBC molecular subgroups. Two independent microarray datasets and a western blot cohort corroborated the unfavourable prognostic role of DSC2 and, together with immunohistochemical analysis on an independent cohort, demonstrated a significantly increased expression of the desmosomal protein in the most aggressive molecular subtypes, namely the aforementioned HER2 positive and TNBC. Our results have further highlighted the potential of DSC2 as a predisposing marker for the development of breast cancer metastases to the brain and lungs, and are in line with a previous work by Landemaine et al. who identified DSC2 as a potential predictive marker for lung metastasis in breast cancer [40]. With the rising incidence of breast cancer cerebral metastases, and the lingering difficulty in treating the disease, the ability to identify high risk patients who would benefit from increased prevention would be of great clinical value. In line with a previous study on brain metastasis samples from patients with different tumour entities, which identified DSC2 as a potential marker for brain metastasis development [27], we found that high DSC2 mRNA expression significantly correlated with an increased risk for cerebral and lung metastases, although for the first localization, this trend could not be validated at a protein level. High DSC2 protein expression was, however, significantly associated with the development of pulmonary metastases [41].

Our findings challenge the self-evident hypothesis that up-regulation of desmosomal proteins leads to a more mechanically cohesive primary tumour, and therefore a less aggressive one. Indeed, a possible explanation for the contrary findings is that enhanced tumour cell aggregation through DSC2 up-regulation is a factor which favours the development of CTC clusters, which have a considerably higher metastatic potency than singular CTC [9, 18]. In various studies, apoptotic morphology was detected in single CTCs, but not within CTC clusters. This finding supports the theory that clustering of CTCs leads to a higher metastatic potential by, for example, increasing the probability of survival in the circulation [11, 42]. Marrella et al. showed that shear stress affects CTC survival in vitro, with CTC clusters being more resistant to shear forces than single CTCs [43]. Increasing shear stress values incrementally caused disaggregation of CTC clusters. Shear stress resistant cells were found to express more DSC2 and DSC1 [31], and were more likely to form clusters. Additionally, a link has been drawn between increased CTC cluster density and size, and increased cluster cell survival in vitro [44]. Additional to an increased resilience, the formation of clusters—in particular those with a very high

density—may lead to reduced chemosensitivity and, thus, a survival advantage compared to single CTCs [12, 44, 45]. Enhanced cell–cell interactions in CTC clusters could also confer resistance to anoikis, a form of apoptosis due to deprivation of cell–cell and cell–matrix contacts [12, 19]. Furthermore, heterogenous cluster formation with immune cells, such as macrophages or leucocytes, may provide a mechanism for immune escape [42]. Collectively, these findings indicate that DSC2 mediated cell adhesion is probably of greater functional importance in later steps of the metastatic cascade, such as survival within the circulation and chemoresistance, rather than in the process of dissolution of future metastatic cells from the primary tumour mass.

In the present study, up-regulation of DSC2 in breast cancer cells led, as expected, to an enhanced cellular aggregation capacity and thus the formation of tight 3D cell clusters, while tumour cell aggregates after DSC2 silencing displayed a looser structure which rapidly dissociated when subjected to mechanical stress. Interestingly, higher DSC2 expressing aggregates showed lower apoptotic rates than the corresponding control clusters when treated with cisplatin and, correspondingly, reduced DSC2 expression significantly enhanced tumour cell response to cisplatin. In contrast, we did not observe any effect of DSC2 up- or down-regulation on the chemosensitivity of both TNBC cell lines cultured as a monolayer, indicating that the DSC2-mediated cohesiveness of the 3D tumour cell clusters is the main reason for the altered chemosensivity. This finding highlights the relevance of in vitro 3D culture models to accurately mimic the in vivo conditions [46]. Tumour cell aggregation significantly influences cell response to cytotoxic drugs, as cells in a spheroid environment are more resistant to radiation and chemotherapeutic agents, a phenomenon known as multicellular resistance (MCR) that has been described for different anticancer drugs, including cisplatin [47]. Possible mechanisms of MCR include signalling-mediated inhibition of apoptosis, an increased proportion of quiescent cells, as well as reduced permeability and, in turn, impeded drug diffusion. Li et al. recently described high DSC2 and PKP1 levels in shear stress-resistant breast and lung cancer, which facilitate cell cluster formation and also activate the PI3K/AKT/Bcl-2–mediated pathway, thereby increasing cell survival [31]. However, the exact mechanism behind the observed DSC2-mediated chemoresistance in our model remains unclear and needs to be elucidated in the context of an ongoing project.

Under 2D culture conditions, up- or down-regulation of DSC2 was found to have only a minor effect on cell migration and invasion, although the tendency of our results is in line with recent studies on adhesion proteins

17

(for example DSG2) and cell migration [25, 48]. No severe impact of increased or decreased DSC2 expression on cell morphology, proliferation or apoptosis could be detected in our 2D cell culture. These findings contrast with diverse reports describing a clear effect of DSC2 down-regulation on 2D proliferation and/or apoptosis in, for example, breast, prostate or oesophageal squamous cell carcinoma in vitro [28, 31, 49], with both a pro- and anti-tumorigenic role being postulated. Thus, the role of DSC2 seems to be entity-specific, or even subtype-specific, as shown in our study with a clear negative prognostic value of DSC2 in HER2 positive and TNBC, yet no impact on survival for patients with luminal breast cancer.

The results of the in vivo metastatic model, even though the size of the experiment did not allow a significant conclusion, clearly underline our hypothesis. Reduced DSC2 tumour expression decreases the amount of viable tumour cells in the blood circulation—CTCs as well as CTC clusters—and, as a consequence, reduces the effective formation of distant metastases. Our results are in line with those recently published by Li et al. showing the relevance of dual expression of DSC2 and PKP1 for cluster formation and survival in circulation in a lung cancer cell line in a tail vein injection model [31].

Conclusions

Our results link high DSC2 expression with the TNBC molecular subtype, a higher breast cancer tumour grade and a significantly shorter disease-free survival. Further, we have been able to highlight the potential predictive value of DSC2 for the development of cerebral and pulmonary metastases. Functionally, DSC2 promotes tumour cell aggregation and, in turn, fosters the formation of tight CTC clusters with high metastatic potential. An interesting possibility for future research would be to expand the DSC2 analyses to circulating tumour cells and clusters, as well as pulmonary breast cancer metastases, in order to further clarify the potential of DSC2 as a breast cancer brain and pulmonary metastases marker for clinical use.

Abbreviations

CTCs	Circulating tumour cells
BBB	Blood–brain barrier
BCBM	Breast cancer brain metastases
BM	Brain metastases
DSC2	Desmocollin-2
SDS	Sodium dodecyl sulphate
WB	Western blot
SI	Stain intensity
PP	Percentage of positive cells
TMA	Tissue microarray
TBST	Tris buffered saline with tween
ABC-complex	Avidin–biotin enzyme complex
DAB	Diaminobenzidin
TBS	Tris-buffered saline
SPSS	Statistical Package for Social Sciences
TNBC	Triple negative breast cancer(s)

Declarations

Ethics approval and consent to participate

All patients gave written approval for the utilisation of their tissue samples and the reviewing of their medical records according to our investigational review board and ethics committee guidelines (Ethik-Kommission der Ärztekammer Hamburg, #OB/V/03). The animal study protocol was approved by the Behörde für Gesundheit und Verbraucherschutz of Freie und Hansestadt Hamburg (N005/2020; 12.03.2020).

Consent for publication

Not applicable.

Competing interests

The authors declare no conflict of interest concerning the presented analysis. IW received speaker´s honoraria outside this work from Amgen, Astra Zeneca, Daiichi-Sankyo, Lilly, MSD, Novar-tis, Pierre Fabre, Pfizer, Roche, and Seagen. VM received speaker's honoraria from Amgen, Astra Zeneca, Daiichi-Sankyo, Eisai, GSK, Pfizer, MSD, Medac, Novartis, Roche, Teva, Seagen, Onkowissen, high5 Oncology, Medscape, Gilead, Pierre Fabre; consultancy honoraria from Hexal, Roche, Pierre Fabre, Amgen, ClinSol, Novartis, MSD, Daiichi-Sankyo, Eisai, Lilly, Sanofi, Seagen, Gilead; institutional research support from Novartis, Roche, Seagen, Genentech and travel grants from Roche, Pfizer, Daiichi Sankyo, Gilead.BS received speaker´s honoraria, travel grants and consultancy honoraria as well as institutional research support outside this work from Eisai, Astra

Author details
[1]Department of Gynaecology, University Medical Center Hamburg-Eppendorf, Martinistraße 52, 20246 Hamburg, Germany. [2]Goethe University, Frankfurt, Germany. [3]Institute for Pathology, Department of Molecular Pathology, University of Basel, Basel, Switzerland. [4]Institute of Neuropathology, University Medical Center Hamburg-Eppendorf, Hamburg, Germany. [5]Institute of Tumor Biology, University Medical Center Hamburg-Eppendorf, Hamburg, Germany. [6]Institute of Experimental Anatomy, University Medical Center Hamburg-Eppendorf, Hamburg, Germany. [7]MSH Medical School of Hamburg, University of Applied Sciences and Medical University, Hamburg, Germany.

References
1. Torre LA, Siegel RL, Ward EM, Jemal A. Global cancer incidence and mortality rates and trends—an update. Cancer Epidemiol Biomarkers Prev. 2016;25(1):16–27.
2. Hess KR, Varadhachary GR, Taylor SH, Wei W, Raber MN, Lenzi R, et al. Metastatic patterns in adenocarcinoma. Cancer. 2006;106(7):1624–33.
3. Kennecke H, Yerushalmi R, Woods R, Cheang MC, Voduc D, Speers CH, et al. Metastatic behavior of breast cancer subtypes. J Clin Oncol. 2010;28(20):3271–7.
4. Laakmann E, Witzel I, Fasching PA, Rezai M, Schem C, Solbach C, et al. Development of central nervous system metastases as a first site of metastatic disease in breast cancer patients treated in the neoadjuvant trials GeparQuinto and GeparSixto. Breast Cancer Res. 2019;21(1):60.
5. Wei S, Siegal GP. Metastatic organotropism: an intrinsic property of breast cancer molecular subtypes. Adv Anat Pathol. 2017;24(2):78–81.
6. Hanahan D, Weinberg RA. Hallmarks of cancer: the next generation. Cell. 2011;144(5):646–74.
7. Lambert AW, Pattabiraman DR, Weinberg RA. Emerging biological principles of metastasis. Cell. 2017;168(4):670–91.
8. Nguyen DX, Bos PD, Massague J. Metastasis: from dissemination to organ-specific colonization. Nat Rev Cancer. 2009;9(4):274–84.
9. Aceto N, Bardia A, Miyamoto DT, Donaldson MC, Wittner BS, Spencer JA, et al. Circulating tumor cell clusters are oligoclonal precursors of breast cancer metastasis. Cell. 2014;158(5):1110–22.
10. Cheung KJ, Ewald AJ. A collective route to metastasis: seeding by tumor cell clusters. Science. 2016;352(6282):167–9.
11. Giuliano M, Shaikh A, Lo HC, Arpino G, De Placido S, Zhang XH, et al. Perspective on circulating tumor cell clusters: why it takes a village to metastasize. Cancer Res. 2018;78(4):845–52.
12. Hou JM, Krebs MG, Lancashire L, Sloane R, Backen A, Swain RK, et al. Clinical significance and molecular characteristics of circulating tumor cells and circulating tumor microemboli in patients with small-cell lung cancer. J Clin Oncol. 2012;30(5):525–32.
13. Krol I, Schwab FD, Carbone R, Ritter M, Picocci S, De Marni ML, et al. Detection of clustered circulating tumour cells in early breast cancer. Br J Cancer. 2021;125(1):23–7.
14. Jansson S, Bendahl PO, Larsson AM, Aaltonen KE, Ryden L. Prognostic impact of circulating tumor cell apoptosis and clusters in serial blood samples from patients with metastatic breast cancer in a prospective observational cohort. BMC Cancer. 2016;16:433.
15. Mu Z, Wang C, Ye Z, Austin L, Civan J, Hyslop T, et al. Prospective assessment of the prognostic value of circulating tumor cells and their clusters in patients with advanced-stage breast cancer. Breast Cancer Res Treat. 2015;154(3):563–71.
16. Wang C, Mu Z, Chervoneva I, Austin L, Ye Z, Rossi G, et al. Longitudinally collected CTCs and CTC-clusters and clinical outcomes of metastatic breast cancer. Breast Cancer Res Treat. 2017;161(1):83–94.
17. Follain G, Herrmann D, Harlepp S, Hyenne V, Osmani N, Warren SC, et al. Fluids and their mechanics in tumour transit: shaping metastasis. Nat Rev Cancer. 2020;20(2):107–24.
18. Cheung KJ, Padmanaban V, Silvestri V, Schipper K, Cohen JD, Fairchild AN, et al. Polyclonal breast cancer metastases arise from collective dissemination of keratin 14-expressing tumor cell clusters. Proc Natl Acad Sci U S A. 2016;113(7):E854–63.
19. Han HJ, Sung JY, Kim SH, Yun UJ, Kim H, Jang EJ, et al. Fibronectin regulates anoikis resistance via cell aggregate formation. Cancer Lett. 2021;508:59–72.
20. Saias L, Gomes A, Cazales M, Ducommun B, Lobjois V. Cell-cell adhesion and cytoskeleton tension oppose each other in regulating tumor cell aggregation. Cancer Res. 2015;75(12):2426–33.
21. Delva E, Tucker DK, Kowalczyk AP. The desmosome. Cold Spring Harb Perspect Biol. 2009;1(2): a002543.
22. Garrod D, Chidgey M. Desmosome structure, composition and function. Biochim Biophys Acta. 2008;1778(3):572–87.
23. Harrison OJ, Brasch J, Lasso G, Katsamba PS, Ahlsen G, Honig B, et al. Structural basis of adhesive binding by desmocollins and desmogleins. Proc Natl Acad Sci USA. 2016;113(26):7160–5.
24. Lee YT. Breast carcinoma: pattern of metastasis at autopsy. J Surg Oncol. 1983;23(3):175–80.
25. Chang PH, Chen MC, Tsai YP, Tan GYT, Hsu PH, Jeng YM, et al. Interplay between desmoglein2 and hypoxia controls metastasis in breast cancer. Proc Natl Acad Sci U S A. 2021;118(3): e2014408118.
26. Hutz K, Zeiler J, Sachs L, Ormanns S, Spindler V. Loss of desmoglein 2 promotes tumorigenic behavior in pancreatic cancer cells. Mol Carcinog. 2017;56(8):1884–95.
27. Saunus JM, Quinn MC, Patch AM, Pearson JV, Bailey PJ, Nones K, et al. Integrated genomic and transcriptomic analysis of human brain metastases identifies alterations of potential clinical significance. J Pathol. 2015;237(3):363–78.
28. Fang WK, Liao LD, Li LY, Xie YM, Xu XE, Zhao WJ, et al. Down-regulated desmocollin-2 promotes cell aggressiveness through redistributing adherens junctions and activating beta-catenin signalling in oesophageal squamous cell carcinoma. J Pathol. 2013;231(2):257–70.
29. Kolegraff K, Nava P, Helms MN, Parkos CA, Nusrat A. Loss of desmocollin-2 confers a tumorigenic phenotype to colonic epithelial cells through activation of Akt/beta-catenin signaling. Mol Biol Cell. 2011;22(8):1121–34.
30. Fang WK, Liao LD, Zeng FM, Zhang PX, Wu JY, Shen J, et al. Desmocollin-2 affects the adhesive strength and cytoskeletal arrangement in esophageal squamous cell carcinoma cells. Mol Med Rep. 2014;10(5):2358–64.
31. Li K, Wu R, Zhou M, Tong H, Luo KQ. Desmosomal proteins of DSC2 and PKP1 promote cancer cells survival and metastasis by increasing cluster formation in circulatory system. Sci Adv. 2021;7(40): eabg7265.
32. Bos PD, Zhang XH, Nadal C, Shu W, Gomis RR, Nguyen DX, et al. Genes that mediate breast cancer metastasis to the brain. Nature. 2009;459(7249):1005–9.
33. Hamester F, Sturken C, Saygi C, Qi M, Legler K, Gorzelanny C, et al. Insights into the steps of breast cancer-brain metastases development: tumor cell interactions with the blood–brain barrier. Int J Mol Sci. 2022;23(3):1900.
34. Nehmann N, Wicklein D, Schumacher U, Muller R. Comparison of two techniques for the screening of human tumor cells in mouse blood: quantitative real-time polymerase chain reaction (qRT-PCR) versus laser scanning cytometry (LSC). Acta Histochem. 2010;112(5):489–96.
35. Hvichia GE, Parveen Z, Wagner C, Janning M, Quidde J, Stein A, et al. A novel microfluidic platform for size and deformability based separation and the subsequent molecular characterization of viable circulating tumor cells. Int J Cancer. 2016;138(12):2894–904.
36. Alix-Panabieres C, Pantel K. Challenges in circulating tumour cell research. Nat Rev Cancer. 2014;14(9):623–31.
37. Lawson DA, Bhakta NR, Kessenbrock K, Prummel KD, Yu Y, Takai K, et al. Single-cell analysis reveals a stem-cell program in human metastatic breast cancer cells. Nature. 2015;526(7571):131–5.
38. Legan PK, Yue KKM, Chidgey MAJ, Holton JL, Wilkinson RW, Garrod DR. The Bovine Desmocollin Family—a new gene and expression patterns reflecting epithelial-cell proliferation and differentiation. J Cell Biol. 1994;126(2):507–18.
39. Hegazy M, Perl AL, Svoboda SA, Green KJ. Desmosomal cadherins in health and disease. Annu Rev Pathol. 2022;17:47–72.

19

40. Landemaine T, Jackson A, Bellahcene A, Rucci N, Sin S, Abad BM, et al. A six-gene signature predicting breast cancer lung metastasis. Cancer Res. 2008;68(15):6092–9.

41. Bryan S, Witzel I, Borgmann K, Oliveira-Ferrer L. Molecular mechanisms associated with brain metastases in HER2-positive and triple negative breast cancers. Cancers. 2021;13(16):4137.

42. Schuster E, Taftaf R, Reduzzi C, Albert MK, Romero-Calvo I, Liu H. Better together: circulating tumor cell clustering in metastatic cancer. Trends Cancer. 2021;7(11):1020–32.

43. Marrella A, Fedi A, Varani G, Vaccari I, Fato M, Firpo G, et al. High blood flow shear stress values are associated with circulating tumor cells cluster disaggregation in a multi-channel microfluidic device. PLoS ONE. 2021;16(1): e0245536.

44. Campenni M, May AN, Boddy A, Harris V, Nedelcu AM. Agent-based modelling reveals strategies to reduce the fitness and metastatic potential of circulating tumour cell clusters. Evol Appl. 2020;13(7):1635–50.

45. Reynolds DS, Tevis KM, Blessing WA, Colson YL, Zaman MH, Grinstaff MW. Breast cancer spheroids reveal a differential cancer stem cell response to chemotherapeutic treatment. Sci Rep. 2017;7(1):10382.

46. Breslin S, O'Driscoll L. The relevance of using 3D cell cultures, in addition to 2D monolayer cultures, when evaluating breast cancer drug sensitivity and resistance. Oncotarget. 2016;7(29):45745–56.

47. Desoize B, Jardillier J. Multicellular resistance: a paradigm for clinical resistance? Crit Rev Oncol Hematol. 2000;36(2–3):193–207.

48. Hapach LA, Carey SP, Schwager SC, Taufalele PV, Wang W, Mosier JA, et al. Phenotypic heterogeneity and metastasis of breast cancer cells. Cancer Res. 2021;81(13):3649–63.

49. Jiang F, Wu P. Regulating DSC2 expression affects the proliferation and apoptosis of prostate cancer cells. Cancer Manag Res. 2020;12:11453–62.

Publisher's Note

Springer Nature remains neutral with regard to jurisdictional claims in published maps and institutional affiliations.

Additional File 1: Supplementary Figures, Material and Methods

Figure S1. DSC2 Microarray Analysis in an independent validation cohort. For validation purpose we used an independent Affymetrix microarray dataset consisting of 572 breast cancer samples from Gene Expression Omnibus (GSE2603, GSE2034, GSE12276) for which detailed information on metastatic localization was available [PMID 19421193].
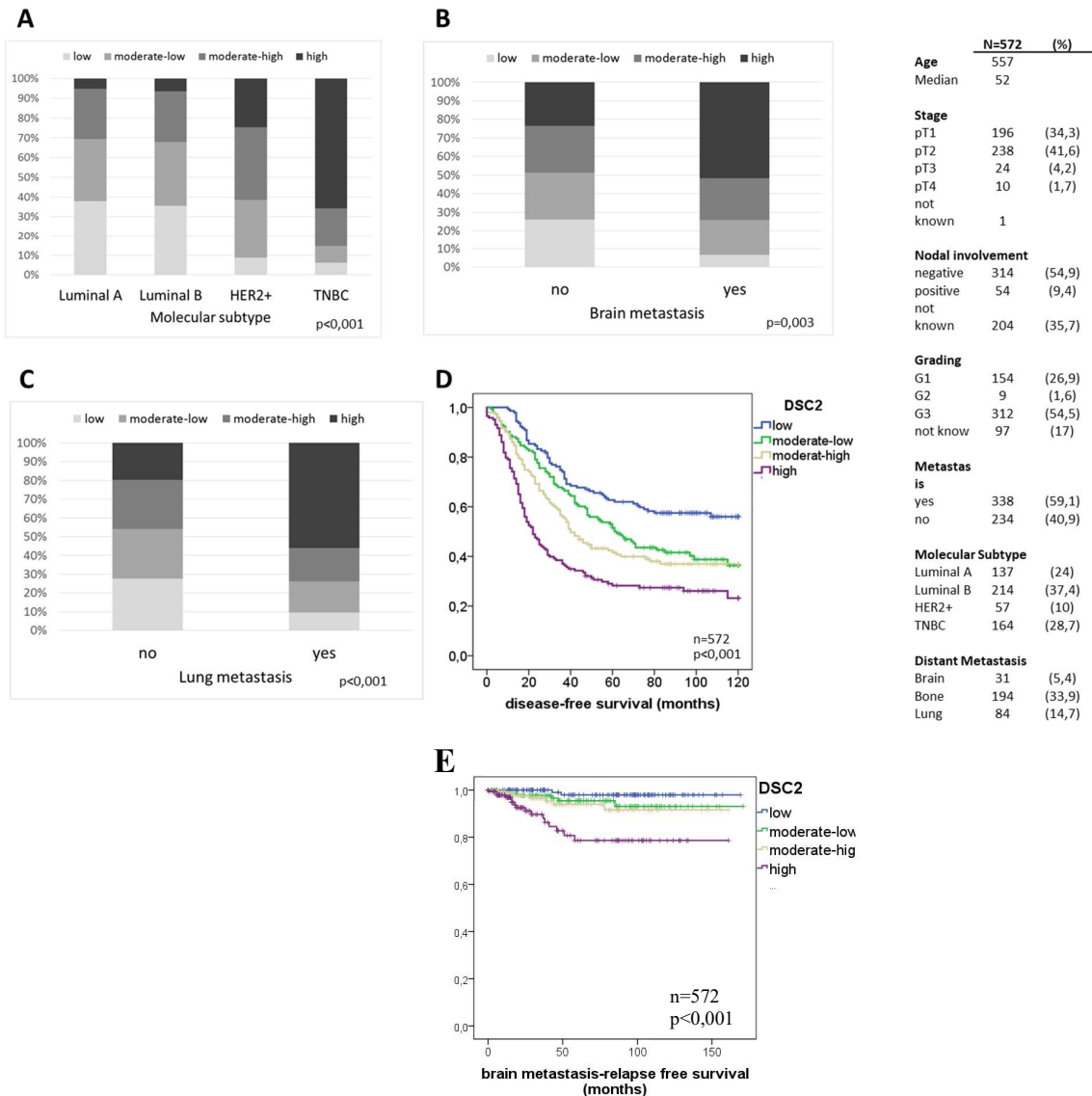
Figure S2. In Western Blot analysis PR- and ER- negativity were significantly associated with high DSC2 protein levels (all bands: left side and upper band: right side)
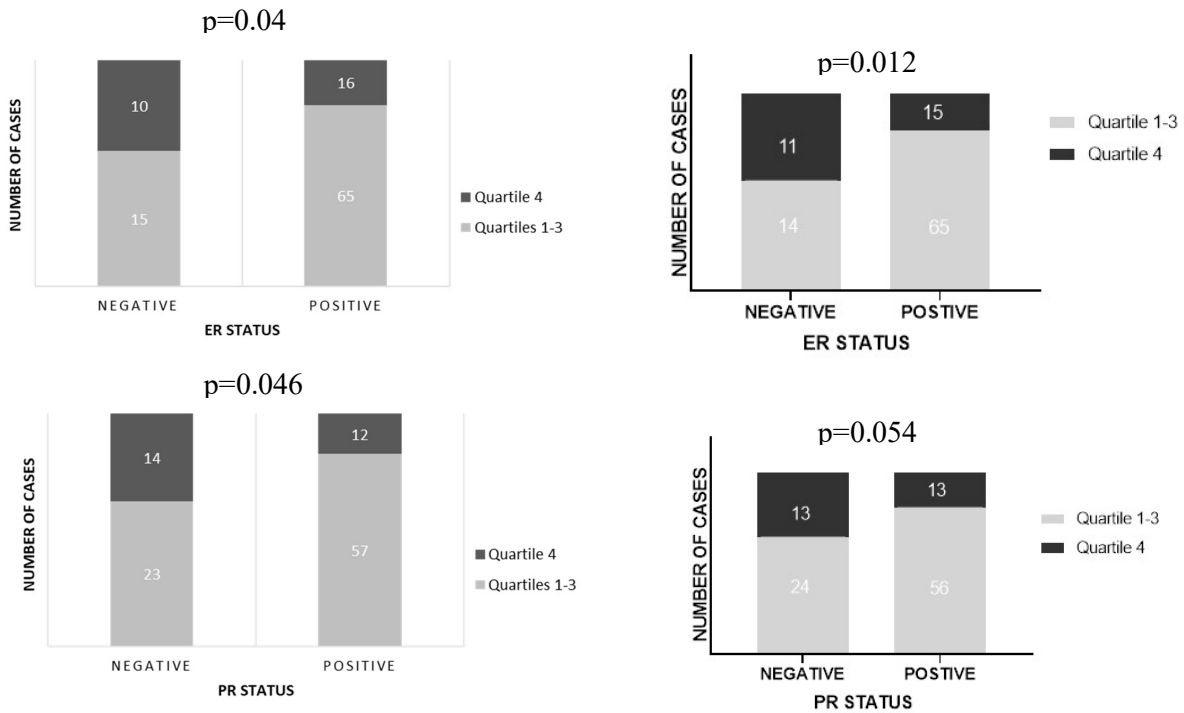
Figure S3. Overexpression of DSC2. (**A**) mRNA level in wild type (WT) MDA-MB-231-BR and after lentiviral transduction with LEGO-iC2-DSC2 and the empty vector (LeGO-iC2). (**B**) Morphology of cell spheroids with MDA-MB-231-BR WT, LeGO-iC2 (empty vector) and LeGO-iC2-DSC2 (DSC2 overexpression) cells, before and after mechanical dissociation.
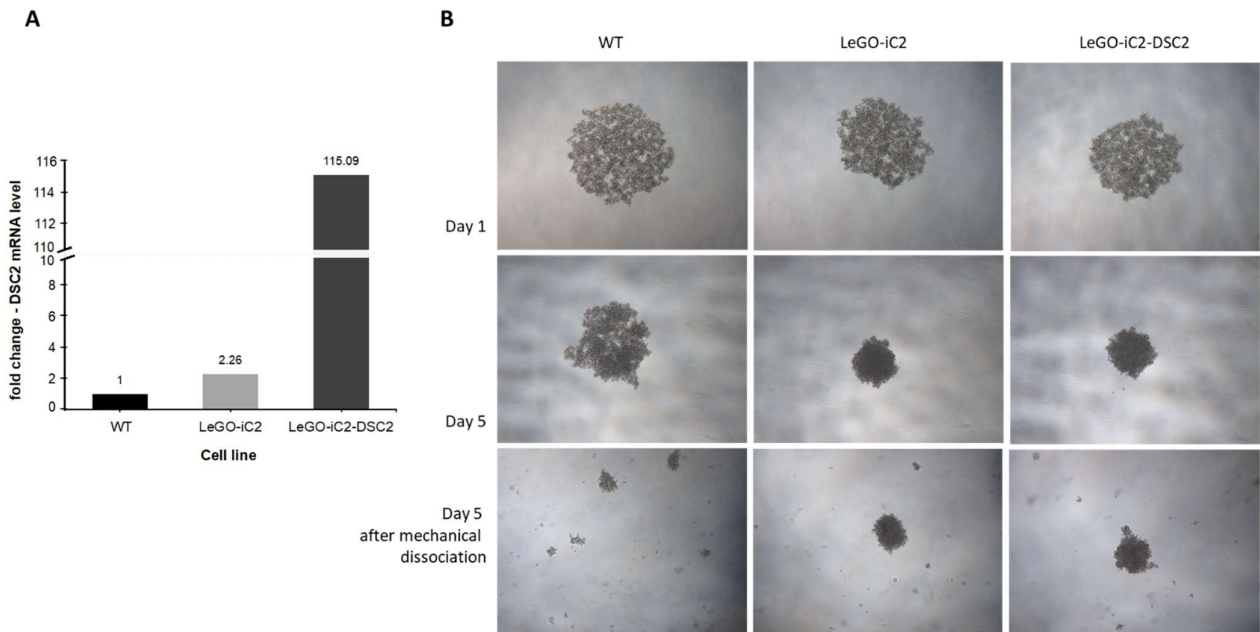
Figure S4. Cisplatin PT-GG staining. **(A)** Exemplary images of immunohistochemical PT-GG staining in MDA-MB231-BR scramble and DSC2 shRNA III after 8h treatment with cisplatin **(B)** Quantification of PT-GG positive and negative cells in MDA-MB231-BR scramble and DSC2 shRNA III after 8h and after 24h treatment with cisplatin **(C)** Exemplary images of immunohistochemical PT-GG staining in MDA-MB231-BR WT, LeGO-iC2 (empty vector) and LeGO-iC2-DSC2 (DSC2 overexpression) after 8h treatment with cisplatin **(D)** Quantification of PT-GG positive and negative cells in MDA-MB231-BR WT, LeGO-iC2 and LeGO-iC2-DSC2 after 8h and after 24h treatment with cisplatin.
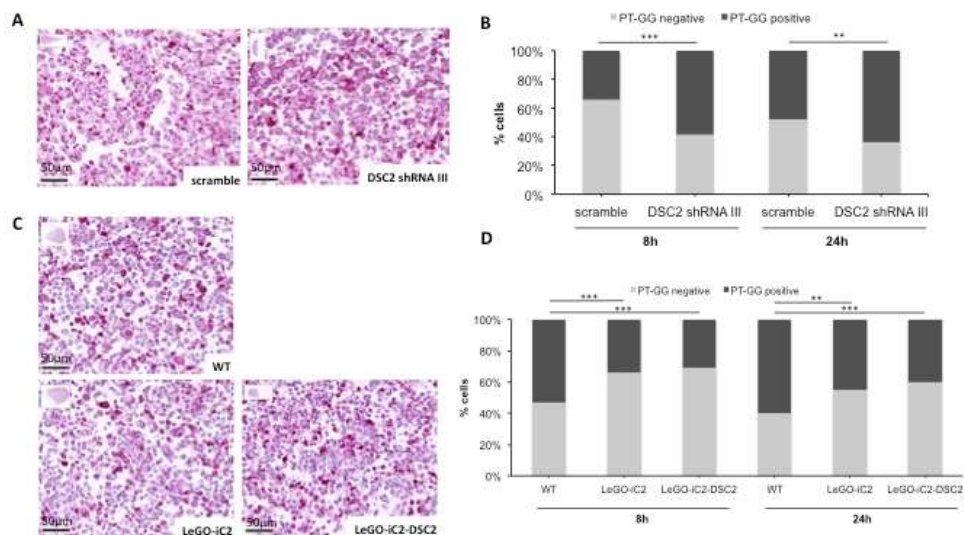
Supplementary Material and Methods

For staining of cisplatin DNA-adducts, slides were deparaffanized, pretreated with FastEnzyme (ZUC059-015, Zytomed, Berlin, Germany) for 5 min and incubated with 1:1000 diluted rat monoclonal PT-GG antibody (Oncolyze, Essen, Germany) for 80 min, respectively at room temperature. After washing, incubation with biotin-conjugated rabbit anti-rat antibody (1:100 dilution in TBS; 312-065-048, JacksonImmuno Research, Ely, UK) followed for 30 min at room temperature. Staining was visualized with streptavidin conjugated Alkaline Phosphatase and Chromogen RED using DAKO Real™ detection System (K5005, DAKO, Glostrup, Denmark) kit according to the manufacturer's instructions. As negative control, rat IgG 2a kappa Isotype Control (14-4321-85, eBioscience, San Diego, CA, USA) was used instead of primary antibody. All slides were counterstained with haematoxylin.

Additional File 2: Patient characteristics Microarray and Western Blot cohorts

Table S1: Patient characteristics	Hamburg Microarray Cohort n=197	Hamburg WesternBlot Cohort n= 111
	n (%)	n (%)
Age (years)		
Median	56.6	56.2
Range	29-94	29-79
Histological Type		
Ductal	140 (71)	75(68)
Lobular	31 (16)	19 (17)
Others	22 (11)	13 (12)
Unknown	4 (2)	2 (2)
Tumor Size (stage)		
< 2cm (pT1)	51 (26)	24 (12)
2-5cm (pT2)	121 (61)	72 (37)
> 5cm (pT3-4)	20 (10)	11 (6)
Unknown	5 (3)	4 (2)
Grade		
I	20 (10)	7 (6)
II	80 (41)	47 (42)
III-Undifferentiated	92 (47)	53 (48)
Unknown	5 (3)	4 (4)
Lymph Nodes		
Negative nodes	136 (69)	70 (63)
Positive nodes	60 (31)	39 (35)
Unknown	1 (0.5)	2 (2)
ER Status		
Positive	148 (75)	81 (73)
Negative	41 (21)	25 (22)
Unknown	8 (4)	5 (5)
PR Status		
Positive	124 (63)	69 (62)
Negative	65 (33)	37 (33)
Unknown	8 (4)	5 (5)
Molecular Subtyp		
Luminal	123 (63)	58 (52)
HER2 +	29 (15)	23 (21)
TN	37 (19)	25 (22)
Unknown	8 (4)	5 (5)
Distant metastases		
All distant metastases	55 (28)	41 (37)
No distant metastases	120 (61)	53 (48)
Unknown	22 (11)	8 (7)
Bone metastases[1]	34 (17)	23 (21)
Lung metastases[1]	28 (14)	23 (21)
Visceral/hepatic metastases[1]	30 (15)	25 (22)
Brain metastases[1]	15 (8)	12 (11)
Follow-up		
Recurrence	72 (37)	51 (46)
No recurrence	105 (53)	52 (47)
Recurence unknown	20 (10)	8 (7)
Died of disease	56 (28)	41 (37)
Died of other course	8 (4)	7 (6)
Alive	126 (64)	60 (54)
Unknown	7 (4)	3 (3)
Median follow-up period (months)	133	142
[1]: multiples included		

Additional File 3: Patient characteristics TMAs

Table S2: Patient characteristics TMAs				
	W18.4062 *n= 105	W18.4025 *n = 47	W18.4026 *n = 58	W18.4023 *n = 16
Tumor Size (stage)				
< 2cm (pT1)	25	17	19	5
2-5cm (pT2)	56	26	31	10
> 5cm (pT3-4)	16	3	7	1
Unknown	8	1	1	0
Grade				
I			1	
II			8	
III-Undifferentiated			45	
Unknown			4	
Lymph Nodes				
Negative nodes	56	16	24	6
Positive nodes	37	25	21	10
Unknown	12	6	13	0
ER Status				
Positive	40	26		12
Negative	24	21		0
Unknown	41	0		4
PR Status				
Positive	40	**20**		12
Negative	24	27		0
Unknown	41	0		4
Molecular Subtyp				
Luminal			2	12
HR+/HER2+	40	26	0	0
HER2 +		16	2	0
TN	24	4	44	0
Unknown	41	11	10	4
Follow-up				
Recurrence	25	6	20	16
No recurrence	61	13	26	0
Recurence unknown	21	28	12	0
Died of disease	12	2	13	8
Alive	68	19	33	8
Unknown	27	26	12	0
Median follow-up period (months)	24,5	57	44	85,5
* analysable biopsies from primary breast cancer samples				

Additional File 4: Correlation between DSC2 mRNA levels and clinical and histopathological parameter

Table S3:
Correlations between DSC2 mRNA levels and clinical and histopathological parameter (p-values)

		DSC2_204750_s_at	DSC2_204751_x_at	DSC2_mean valu
n		200	200	200
Mean		158,2	255,1	206,6
Median		82,3	182,6	140,6
Standard deviation		290,0	234,1	213,8
Variance		84123,9	54808,6	45698,6
Minimum		4,0	8,1	6,1
Maximum		2658,8	1483,5	1610
Percentile	25	36,9	124,1	92,2
	50	82,3	182,6	140,6
	75	174,5	282,0	236,5
pT	χ^2 (Q)	0,061	0,460	0,063
pN	χ^2 (Q)	0,235	0,200	0,072
Metastasis	χ^2 (Q)	0,001	0,671	0,060
Grading	χ^2 (Q)	0,820	0,008	0,070
Histology	χ^2 (Q)	0,372	0,298	0,456
ER	χ^2 (Q)	0,175	< 0,0005	0,0002
PR	χ^2 (Q)	0,555	0,014	0,134
molecular subtype	χ^2 (Q)	0,001	< 0,0005	< 0,0005
distant metastasis	χ^2 (Q)	0,357	0,421	0,393
bone metastasis	χ^2 (Q)	0,647	0,984	0,69
lung metastasis	χ^2 (Q)	0,025	0,092	0,078
visceral metastasis	χ^2 (Q)	0,906	0,633	0,459
skin metastasis	χ^2 (Q)	0,277	0,306	0,030
lymph node metastasis	χ^2 (Q)	0,137	0,628	0,659
locoreg. Metastasis	χ^2 (Q)	0,212	0,890	0,805
cerebral metastasis	χ^2 (Q)	0,575	0,001	0,012
OAS	Cox-regr.	0,004	< 0,0005	0,0001
OAS	Log-rang (Q)	0,400	0,026	0,035
RFI	Cox-regr.	0,001	< 0,0005	0,00001
RFI	Log-rang (Q)	0,056	0,041	0,051
RFI	Log-rang (M)	0,008	0,006	0,021
RFI TNBC	Log-rang (Q)	0,047	0,093	0,005
RFI TNBC	Log-rang (M)	0,005	0,013	0,029

χ^2 (Q): chi-quadrat test using quartiles
Cox-regr.: cox-regression analysis using continous values
Log-rang (Q): log -rang analysis using quartiles
Red-coloured values are significan (< 0,05)
OAS: overall survival
RFI: recurrence-free interval
RFI TNBC: recurrence-free interval in triple-negative breast cancer

Multivariate Cox regression analysis (disease-free survival)

	p value	Hazard ratio	95% CI
DSC2 mean value Q1-3 vs Q4	0,008	2,071	1,207-3,553
pT1	0,394		
pT2	0,444	0,643	0,207-1,993
pT3	0,762	0,851	0,299-2,418
pT4	0,507	1,551	0,424-5,660
pN	0,244	0,739	0,444-1,229
molecular subgroup	0,042	0,632	0,406-0,983

Additional File 5: Correlation between DSC2 mRNA level and protein level

Table S4				

Correlation between protein expression in all detected DSC2 bands				
	Single 110 kDa band	**Upper DB between 93 and 110 kDa**	**Lower DB between 60 and 85 kDa**	**All bands**
Single 110 kDa band	-	**r=0.936** S_ρ=0.936 *P*<0.000	**r=0.646** S_ρ=0.646 *P*<0.000	**r=0.754** S_ρ=0.756 *P*<0.000
Upper DB between 93 and 110 kDa	**r=0.646** S_ρ=0.646 *P*<0.000	-	**r=0.676** S_ρ=0.677 *P*<0.000	**r=0.804** S_ρ=0.805 *P*<0.000
Lower DB between 60 and 85 kDa	**r=0.936** S_ρ=0.036 *P*<0.000	**r=0.676** S_ρ=0.677 *P*<0.000	-	**r=0.873** S_ρ=0.874 *P*<0.000
All bands	**r=0.754** S_ρ=0.756 *P*<0.000	**r=0.804** S_ρ=0.805 *P*<0.000	**r=0.873** S_ρ=0.874 *P*<0.000	-

Correlation coefficients; r=Pearson Correlation, S_ρ=Spearman's rho. *P*=*P*-value. Statistically significant *P*-values are highlighted. DB=double band. Protein expression values were divided into quartiles prior to statistical analysis. UPA497 was used as the positive control for all calculations.

Correlation between DSC2 mRNA (Microarray Data) and protein (WB Data) expression values				
	Single 110 kDa band	**Upper DB between 93 and 110 kDa**	**Lower DB between 60 and 85 kDa**	**All bands**
mRNA	**r=0.431** S_ρ=0.431 *P*<0.0001	**r=0.548** S_ρ=0.547 *P*<0.0001	**r=0.423** S_ρ=0.421 *P*<0.0001	**r=0.440** S_ρ=0.440 *P*<0.0001

Correlation coefficients; r=Pearson Correlation, S_ρ=Spearman's rho. *P*=*P*-value.

2 Summary of the Publication

2.1 Background

Breast cancer is the most common malignancy in females worldwide, affecting approximately 12% of all women in their lifetime (Sung, Ferlay et al. 2021). The disease prognosis varies significantly between breast cancer patients, depending heavily on tumour stage, histological classification, molecular subtype and gene expression profiling at the time of diagnosis and therapy commencement (Schnitt 2010). Breast cancer stage is classified using the TNM staging system, which takes primary tumour size and localisation (T, tumour), as well as spread to lymph nodes (N, node) and distant organs (M, metastases) into account. In the past decades, we have observed a significant improvement in the prognosis of this disease, owing to advancements in diagnostic tools and therapeutic agents, as well as an increased public awareness for the disease and the importance of breast cancer screening. The resulting increase in overall survival has correspondingly led to a rise in the incidence of tumour relapse and metastatic breast cancer spread, augmenting the importance of research, and ensuing therapeutic advancements, in this field (Winters, Martin et al. 2017).

Cancer metastases develop when individual tumour cells or tumour cell clusters separate from the primary tumour, spreading locally or travelling via the bloodstream (hematogenic spread) or lymphatic system (lymphatic spread) to distant organs. Hematogenous metastases of breast cancer predominantly form in bone, lung, liver, and brain tissue (Liang, Zhang et al. 2020).

Understanding the factors which influence the effectiveness and pattern of metastatic spread is vital in the combat of metastatic breast cancer. For example, past research has shown that metastasis is strongly influenced by the tumour's molecular subtype; triple negative (TNBC) and HER2-positive subtypes typically metastasise to the brain and lungs, luminal A and B subtypes commonly metastasise to bone, and liver metastases are predominantly observed in HER2-positive cases (Smid, Wang et al. 2008, Soni, Ren et al. 2015, Bartmann, Wischnewsky et al. 2017). Furthermore, the propensity of tumour cells to form circulating tumour cell clusters (CTC clusters), rather than remaining singular circulating tumour cells (CTCs), appears to influence their survival in the blood stream/ lymphatic system, and thus their metastatic potential (Klotz, Thomas et al. 2020). CTC clusters are cell aggregates of up to 50 tumour cells, which are up to 50-fold more likely to form metastases than single CTCs (Aceto, Bardia et al. 2014).

Recent research into desmosomal proteins, specifically their roll in cell aggregation and adhesion, has highlighted a potential association between increased desmosome density and improved formation of CTC clusters, and thus, metastases (Aceto, Bardia et al. 2014, Saias, Gomes et al. 2015). Desmosomes are dynamic cell junctions which form a vital component of the intercellular scaffolding between neighbouring epithelial cells, enabling intercellular adhesion and epithelial integrity (Al-Jassar, Bikker et al. 2013). For example, high plakoglobin expression levels have been detected in CTC clusters (Xie, Hu et al. 2020). Another recent study has associated the desmosomal protein desmoglein 2 with a poorer prognosis and higher risk of recurrence in breast cancer patients. Their results suggest that hypoxia induced desmoglein 2 expression increases the prevalence of CTC clusters (Chang, Chen et al. 2021).

This study focused specifically on the role of the transmembrane proteins desmocollin 2 (DSC2), belonging to the cadherin superfamily, and plakophilin 1 (PKP1), a member of the arm-repeat (armadillo) family, in breast cancer metastases formation (Image 1). DSC2 has been studied in the context of other cancer entities and here it has been shown that high DSC2 expression increases cell proliferation, invasion (Fang, Liao et al. 2013) and aggregation (Fang, Liao et al. 2014, Saias, Gomes et al. 2015). PKP1 proteins are located in cell desmosomes and the nucleoplasm, and are involved in the linking of cadherins to intermediate filaments in the cytoskeleton. As a desmosome stabiliser, PKP1 plays an important role in stratified and complex epithelia, with PKP1 gene mutations leading to the well described skin fragility syndrome (South 2004). Furthermore, both PKP1 down- and upregulation has been associated with various forms of cancer and metastasis (Yang, Fischer-Keso et al. 2015, Haase, Cui et al. 2019, Martin-Padron, Boyero et al. 2020). However, the roles of DSC2 and PKP1 specifically in breast cancer and in the formation of breast cancer metastases remain largely unknown.
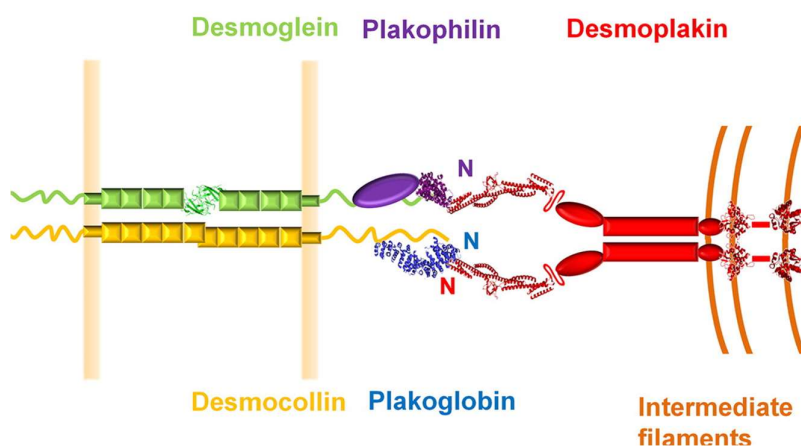

Image 1: Architectural unit of the desmosome.

Source: adapted from the graphical abstract from Al-Jassar, C., H. Bikker, M. Overduin and M. Chidgey (2013). "Mechanistic basis of desmosome-targeted diseases." J Mol Biol 425(21): 4006-4022.

2.2 Study objectives

Preceding microarray analyses of DSC2 and PKP1 in 194 breast cancer mRNA samples (cohort A) highlighted their potential prognostic value, with mRNA expression significantly correlating with an increased risk for brain metastases. The aim of this doctoral research study was to investigate the expression of DSC2 and PKP1 at a protein level in primary breast cancers and, where available, their brain metastasis counterparts, in order to verify the microarray analysis findings and assess their involvement in breast cancer progression and the development of breast cancer metastases.

2.3 Methods

2.3.1 Western Blot

Tissue samples from a total of 110 patients (cohort B) where collected and used to create protein lysates for western blot analyses. Of these, a total of 12 patients developed brain metastasis.

For the western blot analyses, volumes of tumour lysates containing 20 µg of total protein were loaded per well. The proteins were separated via gel electrophoresis on 10% polyacrylamide gels (11% glycerin, distilled water, 10% SDS and 10% acrylamide) and transferred to polyvinylidene difluoride membranes (Merck Millipore KGaA Darmstadt, Germany). Filters were blocked in Roche blocking reagent solution. Primary antibodies diluted in a 1:10 solution of blocking reagent and TBST (TBS: 50mM Tris, 150mM NaCl, pH 7.6 with 10% TWEEN 20) were applied and membranes were incubated over night at 4°C. Filters were washed with TBST and secondary antibodies - diluted in blocking reagent and TBST (1:10) - were applied for 1 hour at room temperature. Subsequent to washing with TBST, bound antibodies were visualised using a chemiluminescent reagent (SuperSignal ® West Pico chemiluminescent Substrate, Thermo Scientific, Rockford, USA). Light emission was detected using FUJI-super RX medical X-ray films (FUJI, Tokyo, Japan). Protein band intensities were quantified using a calibrated densitometer (GS-800 Imaging Densitometer, Bio-Rad, Munich, Germany).

The following antibodies were utilised in the western blot detection process for DSC2: mouse monoclonal anti-DSC2 IgG (Millipore, MABT411) dilution 1:1,000, mouse monoclonal anti-β-Actin (C4) (Santa Cruz Biotechnology, sc-47778) dilution 1:2,000 and goat anti-mouse IgG-HRP (Santa Cruz Biotechnology, sc-2055) dilution 1:8,000.

The following antibodies were utilised in the western blot detection process for PKP1: mouse monoclonal anti-PKP1 IgG (Santa Cruz Biotechnology, sc-33636) dilution 1: 200, mouse monoclonal anti-β-Actin (C4) (Santa Cruz Biotechnology, sc-47778) dilution 1:2,000 and goat anti-mouse IgG-HRP (Santa Cruz Biotechnology, sc-2055) dilution 1:8,000.

Protein lysates from the breast cancer cell line T47D and the breast cancer lysate UPA 497 were used as positive controls for DSC2. Protein lysates from the breast cancer cell line MCF7 and breast cancer sample T1513 from the patient cohort B were used as positive controls for PKP1. Positive control expression was defined as 100% for the purpose of standardisation. Protein expression values were also normalised using the loading control β-Actin.

2.3.2 Immunhistochemistry

Immunohistochemical analyses were performed on primary breast cancer and cerebral metastases samples in order to qualitatively assess the localisation and range of DSC2 and PKP1 expression between varying breast cancer patients and tumour modalities. The samples used in the analyses included primary breast cancer samples from patients with or without brain metastases. In the cases of metastatic breast cancer to the brain, the corresponding brain metastases samples were also analysed.

Furthermore, tissue microarrays (TMAs) of primary breast cancer and brain metastases samples were analysed.

Paraffin embedded tissue samples were deparaffinised in xylene and subsequently re-hydrated in a descending alcohol series, culminating in distilled water. Antigen damasking was achieved in citrate buffer (10 mM) heated in the microwave until boiling, and then for 23 minutes at 90°C in a kitchen steamer. Endogenous peroxidase activity was blocked with 0.5% H_2O_2.

DSC2 sections were incubated at 4°C overnight with the primary antibody (Rabbit anti-DSC2, HPA 012615 von Sigma Aldrich) diluted 1:400 in antibody diluent (S0809, DAKO, CA, USA). Isotype (anti-rabbit IgG, sc-2027, Santa Cruz) and negative control slides (pure antibody diluent) were incubated at 4°C overnight. Incubation with the secondary antibody (anti-rabbit IgG, BA-10000, Vector) occurred at room temperature for 30 minutes.

PKP1 sections were incubated at 4°C overnight with the primary antibody (mouse anti-PKP1, sc-33636 von Santa Cruz Biotechnology,) diluted 1:100. Isotype and negative control slides were simultaneously incubated at 4°C overnight (anti-mouse IgG, X0931, DAKO and pure antibody diluent respectively) and incubation with the secondary antibody (anti-mouse IgG, BA-2000, Vector) occurred at room temperature for 30 minutes.

TBS (5 mM Tris, 15 mM NaCl, pH 7.6) was used for all washing steps. Enzymatic detection of the proteins was achieved using the VECTASTAIN Elite ABC-HRP kit (30 min at room temperature), followed by the peroxidase substrate kit (DAB, SK-4100, Vector). The nuclei were counterstained with hematoxylin (Papanicolau's solution 1a Harris' hematoxylin solution,1.09253.0500, Merck, Darmstadt, Germany or Hem alum solution acid acc. to Meyer, T865.2, Carl Roth, Karlsruhe, Germany). Following dehydration in an ascending alcohol series and xylene, the sections were mounted (Eukitt, 03989, Sigma Aldrich, Deutschland) and visualised using a light microscope (Axioskop 40, Carl Zeiss Imaging Solutions).

The expression and localisation of DSC2 and PKP1 were assessed by two investigators independently. Scores were awarded for stain intensity (SI, 0 = negative, 1 = weak, 2 = moderate, 3 = strong) and homogeneity (percentage of positive tumour cells, 0 = 0%, 1 = <19%, 2 = 20-49%, 3 = 50-79%, 4 = 80-100%). Additional staining of blood vessels and/or the extracellular matrix was also noted.

2.3.3 Statistical Analyses

All statistical analyses were performed using SPSS Statistics version 24 for Windows (IBM, Armonk, NY, USA). Correlations between mRNA levels (microarray data, cohort A) and protein levels (western blot data, cohort B) were assessed using two-sided Pearson tests. Chi-square tests were used to correlate mRNA and protein expression with the following clinical and pathological parameters; histological grading (G1/ G2/ G3), molecular subtype (Luminal/ HER2 positive/ TNBC), oestrogen receptor (ER) and progesterone receptor (PR) status (positive/ negative) and the presence of metastases (bone/ lung/ visceral/ brain/ loco-regional). Kaplan-Meier estimates and the log-rank test were used to analyse disease-free and overall survival. The associated hazard ratios for the multivariate analyses were determined by Cox regression. Probability

values (*p*-value) ≤ 0.05 were considered to be statistically significant.

2.4 Results

2.4.1 Desmocollin 2 - Western Blot Analyses

From the microarray cohort of 197 tumour samples (cohort A), a total of 110 samples (cohort B) were tested at a protein level using western blot. According to the literature and as described in the biological information provided by the antibody manufacturer, the molecular weight of the DSC2 protein is 110 kDa. As expected, most samples presented a correspondingly weighted band. However, in all samples, one or more additional bands were detected by the anti-DSC2 antibody (Figure 2A of the manuscript). These bands most often presented as two double band sets between 60 and 85 kDa, and 93 and 110 kDa. All of the 110 samples were at least lightly positive for one of these double band sets.

In order to clarify the nature of these unexpected bands, the intensity of each singular band and each double band set was quantified by densitometry. The Pearson correlation coefficient between the single band (110 kDa) and the double band (93 -10 kDa) was r = 0.936, and that between both double band sets was r = 0.676 (both p < 0.0000; Supplementary table S4 of the manuscript). Furthermore, all bands showed a significant and at least moderate correlation with the DSC2 mRNA expression determined via microarray analyses (Pearson correlation coefficient r > 0.4; p < 0.001; Supplementary table S4 of the manuscript). On the basis of these results, it can be assumed that all bands are either isoforms of DSC2, or resultant of posttranslational modifications, such as glycosylation. All subsequent analyses are, for the purpose of simplicity, confined to the assessment of the upper 110 kDa band and the collective assessment of all detected DSC2 bands, although similar results were obtained from analyses of each individual band, as well as each double band set.

Western blot analyses showed broad variations in primary breast cancer DSC2 levels and verified a correlation between DSC2 expression at an mRNA and protein level.

The protein expression analyses using our western blot cohort (cohort B, n = 110 highlighted a broad range of DSC2 protein expression in primary breast cancer samples, varying between low and very high expression. In order to better compare DSC2 expression between the samples, and for the purpose of clarity, the intensity values detected by densitometry were grouped into four equal quartiles representing no/low, low-moderate, moderate, and high protein expression. When comparing the microarray and western blot data, a significant correlation between DSC2 expression at an mRNA and protein level was observed for all bands (Pearson correlation coefficient r > 0.4; p < 0.001; Supplementary table S4 of the manuscript). This supports the hypothesis that all bands are isoforms or modified DSC2 proteins, as mentioned above.

High DSC2 expression was significantly associated with the triple negative breast cancer molecular subtype and an increased risk for pulmonary metastases.

The western blot results also validated the significant relationship between high DSC2 expression and the TNBC molecular subtype (p = 0.017; Figure 2B of the manuscript) which was seen at an mRNA level in the microarray analyses. This association was further substantiated by the findings that PR- and ER- negativity were each individually significantly associated with high DSC2 levels (all bands: p = 0.046 and p = 0.04, upper band: p = 0.054 and 0.012 respectively; Supplementary figure S2 of the manuscript). High DSC2 expression was also significantly associated with an increased risk of pulmonary metastases (all bands: p = 0.049, upper band: p = 0.052; Figure 2C of the manuscript). No significant association between high DSC2 levels and increased cerebral metastases could be observed at a protein level in our cohort; an albeit insignificant trend to this effect was, however, observed (all bands: p = 0.405, upper band: p = 0.42).

Patients with moderate to high DSC2 expression levels experienced a significantly shorter disease-free survival than patients whose tumours expressed no or little DSC2.

Patients whose tumours possessed increased levels of DSC2 (Quartiles 2, 3 and 4) sustained a significantly shorter disease-free survival period in comparison to patients with low DSC2 expression (all bands: p = 0.049, upper band: p = 0.157; Figure 2D of the manuscript). No significant trend was observed between the patient's overall survival and the level of DSC2 expressed in her tumour (p = 0.112; Figure 3G of the manuscript).

2.4.2 Desmocollin 2 - Immunohistochemical Analyses

To further validify our findings at a protein level and identify the localisation of DSC2 in breast cancer and brain metastases tumour tissue, immunohistochemical staining was carried out on a variety of primary breast cancer and breast cancer brain metastases sections, as well as TMAs of primary breast cancer and brain metastases samples. Representative DSC2 staining results are shown in figures 1A-D. DSC2 expression was observed exclusively in tumour cells in all samples. Within both primary breast cancer and brain metastases tumour cells, DSC2 was located in the cellular membrane or the cytoplasm. The cell nucleus was uniformly negative for DSC2 (Figures A and C).
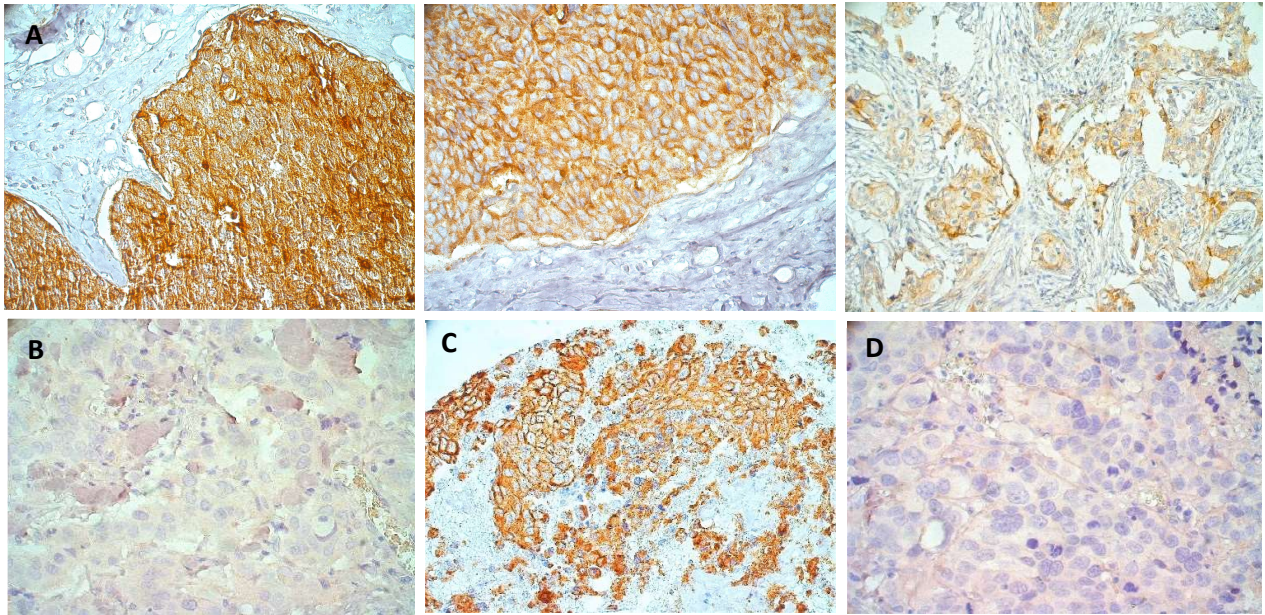
Figure 1: Desmocollin 2 immunohistochemistry in primary breast cancer and breast cancer brain metastases samples. (A) Exemplary images showing the range of DSC2 expression in primary breast cancer samples; strong, membranous, and cytoplasmic staining (*left*), strong membranous staining (*middle*) and moderate, membranous, and cytoplasmic staining (*right*). (B) DSC2 negativity in a breast cancer brain metastases sample. (C) Exemplary image showing strong membranous and cytosolic DSC2 expression in a tissue microarray breast cancer brain metastasis sample. (D) DSC2 negativity in a tissue microarray breast cancer brain metastases sample.

2.4.3 Plakophilin 1 - Western Blot Analyses

A single PKP1 band was detected at 75 kDa (Figure 2). PKP1 expression was assessed semi-quantitively and assigned to four categories (no = 1, weak = 2, moderate = 3, and strong expression = 4). Bands allocated to group 4 were of equal or greater density to the positive control T1513. The results show a moderate and significant correlation between the PKP1 mRNA expression determined via microarray analyses and PKP1 protein expression determined via western blot analyses (Pearson correlation coefficient r = 0.697; p = 0.000).
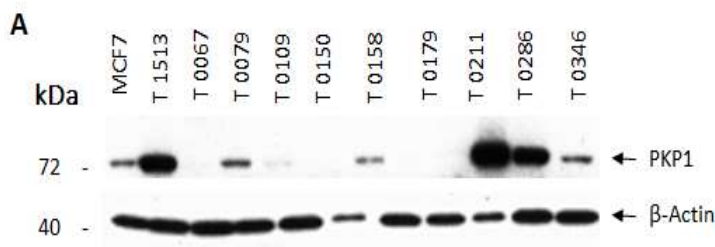

Figure 2: Representative western blot showing PKP1 expression in a range of primary breast cancer samples. Protein lysates from the breast cancer cell line MCF7 and the breast cancer sample T1513 were used as positive controls for PKP1. A single PKP1 band was detected at 75 kDa. β-actin protein expression was quantified as a loading control.

Increased PKP1 expression was significantly associated with an increased incidence of locoregional and pulmonary metastases, as well as a reduced disease-free survival for breast cancer patients.

The western blot analyses (cohort B, n = 110) showed a significant association between tumours with moderate or high PKP1 levels and the development of both loco-regional (p = 0.015; Figure 3A) and pulmonary metastases (p = 0.040; Figure 3 B). Furthermore, patients whose tumours contained high PKP1 levels had a significantly shorter disease-free survival (p = 0.007; Figure 3C). A trend, although statistically insignificant, could be observed between positive PKP1 expression and decreased overall-survival (p = 0.306; Figure 3D).

Further western blot results

The western blot results show a possible association between increased PKP1 expression and estrogen receptor (ER) negativity (p = 0.043), as well as higher tumour grading (p = 0.064). No significant association could be shown between PKP1 expression and the following clinicopathological parameters: cerebral metastases (p = 0.555), PR-status (p = 0.385), pN status (p = 0.573) and pT number (p = 0.499).
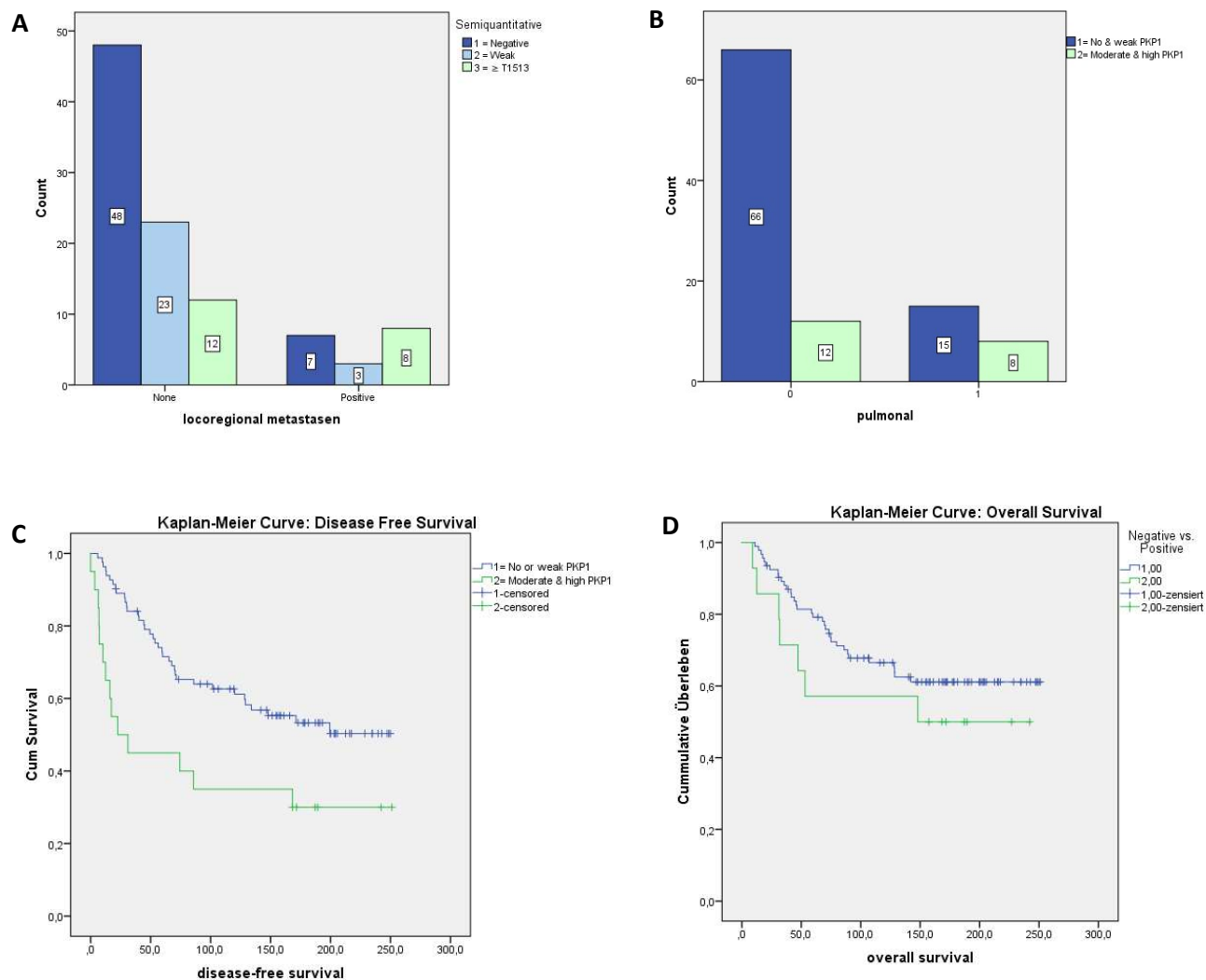
Figure 3. Semi-quantitative expression of PKP1 in primary breast cancer lysates and its correlation with clinicopathological variables. (A) Tumours with high PKP1 levels are significantly associated with increased locoregional metastases development (p = 0.015). (B) A significant association was observed between high PKP1 expression and the development of pulmonary metastases (p = 0.04) (C) Disease-free survival in accordance with PKP1 expression levels. Patients with a moderate to high PKP1 expression have a significantly shorter disease-free survival compared with patients whose tumours possess no or little PKP1 (p = 0.007). (D) The trend observed between increased PKP1 expression and a reduced overall survival was not statistically significant (p = 0.306).

2.4.4 Plakophilin 1 - Immunohistochemical Analyses

The immunohistochemical staining located PKP1 not only in some tumour cells, but also myoepithelium, blood vessels and tumour-associated extracellular matrix (Figures A-C). Within tumour cells, positive PKP1 staining was strictly cytoplasmic; no nuclear staining for PKP1 was observed. Cytoplasmic PKP1 staining was also observed in some breast cancer brain metastases (Figures 4D and E). Nonspecific background staining was observed in a variety of samples (Figure F).
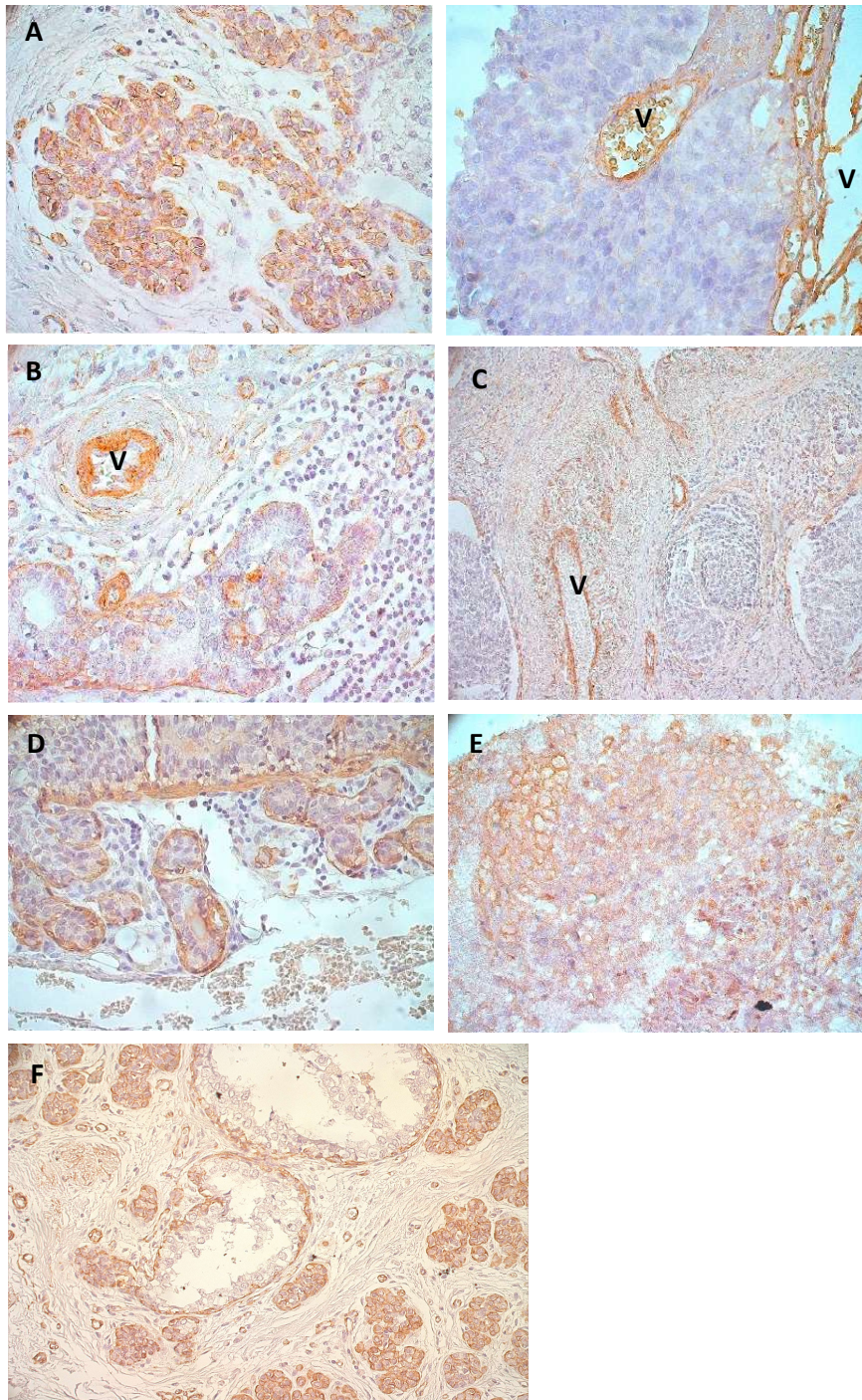
Figure 4: Plakophilin 1 immunohistochemistry in primary breast cancer and breast cancer brain metastases samples. (A) Exemplary images showing PKP1 staining in primary breast cancer samples; moderate cytoplasmic staining and negative nuclear staining (*left*), negative cytoplasmic and negative nuclear staining (*right*). (B, C) PKP1 was also detected in myoepithelial cells, blood vessels and tumour-associated extracellular matrix. (D) PKP1 expression in a primary breast cancer sample from a patient without brain metastases. (E) PKP1 expression in a tissue microarray breast cancer brain metastases sample. (F) Exemplary image showing presumably nonspecific PKP1 background staining, with almost all tumour cells and extracellular tissues stained "positive" for PKP1.

2.5 Discussion

Desmosomal proteins are important structural components which enable intercellular adhesion, and maintain epithelial integrity, acting as the scaffolding linking adjacent cells with the cytoskeleton (Al-Jassar, Bikker et al. 2013). In recent years, desmosomal proteins and, specifically, their role in cancer development and spread, have increasingly been a focus for cancer research. Both tumour-enhancing and tumour-suppressive qualities have been attributed to these proteins in a variety of primary tumour entities, including oesophageal, lung and prostate cancer (Fang, Liao et al. 2014, Yang, Fischer-Keso et al. 2015, Haase, Cui et al. 2019, Martin-Padron, Boyero et al. 2020, Hegazy, Perl et al. 2022). Specifically in the field of breast cancer research, the desmosomal proteins desmocollin 2 (DSC2), plakophilin 1 (PKP1), plakoglobin and desmoglein 2 have each, in recent studies, been associated with an increased formation of circulating tumour cell (CTC) clusters, an augmented metastasis risk und, thus, a poorer prognosis (Aceto, Bardia et al. 2014, Chang, Chen et al. 2021, Li, Wu et al. 2021). For example, Aceto et al. were able to show that plakoglobin knockdown causes disaggregation of CTC clusters, leading to compromised metastatic efficacy in animal models (Aceto, Bardia et al. 2014). This doctoral thesis focused on the proteins DSC2 and PKP1, specifically investigating their expression patterns in primary breast cancer and brain metastases samples, in order to gain further insight into their role in the progression of primary and metastatic breast cancer.

Preliminary microarray analyses had, prior to this study, been performed to assess DSC2 and PKP1 expression at an mRNA level. Here, an association between high DSC2 and PKP1 mRNA levels, and increased disease progression and metastases was observed, forming the foundation of this research, which focused on their expression and influence at a protein level.

When correlated with clinical and histopathological patient data, the western blot results for DSC2 similarly suggest a significant influence of DSC2 expression on disease progression and prognosis. Tumours with increased DSC2 levels were most commonly of the TNBC subtype. HER2 positive and luminal tumours were more likely to express moderate to low DSC2 levels. The western blot results also support the observation that DSC2-rich tumours were more likely to form pulmonary metastases, presenting the potential of DSC2 as a predictive marker for pulmonary metastases risk assessment. These results are in line with the findings from Landemaine et al., which also linked increased DSC2 expression with a higher lung metastases risk in breast cancer patients (Landemaine, Jackson et al. 2008). The significant association between increased DSC2 expression and increased cerebral metastases risk observed at an mRNA level could not, however, be validated at a protein level, presumably due to the small sample size of brain metastases in our western blot cohort (n = 12). An albeit statistically insignificant trend to the effect was, however, observed, underlining the need for further research to substantiate the possible correlation between DSC2 expression and cerebral metastases. Furthermore, increased DSC2 expression led to a shorter disease-free survival, presumably due to the increased metastatic potential of DSC2 expressing primary tumours. Similar findings were published by Li et al., correlating high DSC2 (and PKP1) expression in breast and lung cancer samples with a shorter overall survival and worse disease progression (Li, Wu et al. 2021). Han et al. similarly reported that high DSC2 expression levels in their breast and lung cancer cohorts was significantly correlated with a poorer overall survival (Han, Sung et al. 2021).

The DSC2 immunohistochemistry results mirror the observation seen in our western blot data that DSC2 expression varies between no and strong expression, and pinpoint DSC2 exclusively in tumour cells. No DSC2 expression could be detected in the brain metastases samples. Further research is required to validate this finding. The lack of DSC2 positivity may, for example, be due to poor sample quality or an incorrect staining procedure for the tested brain metastases samples.

On the basis of these preliminary results, the immunohistochemical staining protocol for DSC2 was improved and subsequent staining experiments on primary breast cancer samples were performed by the co-authors of the paper, the results of which were included in the final publication. These analyses could confirm a significant association between increased DSC2 expression and the TNBC molecular subtype (p = 0.046; Figure 2H in manuscript). Representative examples of DSC2 staining in the luminal, HER2 positive and TNBC molecular subtypes can be seen in figures 2I-N of the manuscript.

The western blot results for PKP1 showed that increased PKP1 protein expression was associated with an increased risk for locoregional and pulmonary metastases, as well as a significantly shorter disease-free survival. Similarly to DSC2, the significant association between increased PKP1 mRNA and increased cerebral metastases observed in the microarray data could not be validated at a protein level. As mentioned above, the small sample size (n = 12) is a likely explanation for this result.

Immunohistochemical staining detected PKP1 not only in tumour tissue, but also in myoepithelial cells, blood vessels and the extracellular matrix. No significant trends or associations could be determined in the semi-quantitative analyses of the staining. This is presumably due to nonspecific (background) staining, which can bis falsely misinterpreted as a positive result (Ward and Rehg 2014), and must be acknowledged as a limitation of this research project. Future analyses should focus on establishing a specific PKP1 staining protocol, including testing alternative PKP1 antibodies.

One possible explanation for the comparatively superior metastatic capability and overall poorer prognosis of DSC2- and PKP1-expressing breast cancers and is that the desmosomal proteins play an integral role in the formation of robust CTC clusters which, as previously mentioned, are substantially more metastasis prone than singular CTCs.

CTC clusters have been shown to be more resistant to chemotherapeutic agents then individual tumour cells, as the 3D structure reduces drug exposition to centrally located tumour cells (Hou, Krebs et al. 2012, Schuster, Taftaf et al. 2021). This phenomenon, known as multicellular resistance (MCR), has been described for various anticancer drugs – pertaining to breast cancer, most notably cisplatin - and has been a significant focus point for cancer research over the past decades. New therapeutic drugs must circumvent MCR, for example by disrupting the intercellular connection between circulating tumour cells (Desoize and Jardillier 2000).

Another possible mechanism for the enhanced survival of CTC clusters is the protection against shear forces offered by their 3D structure. *In vitro* experiments performed by Marrella et al. showed a higher resistance to shear forces in CTC clusters than singular CTCs (Marrella, Fedi et al. 2021). Li et al. showed that shear stress resistant breast and lung cancer cells express up to 5.3-fold more DSC2 and PKP1,

facilitating the formation of CTC clusters in circulation and increasing cell survival (Li, Wu et al. 2021).

The survival advantage of CTC clusters in circulation may also relate to a decrease in apoptotic tendencies, when compared to single CTCs (Giuliano, Shaikh et al. 2018, Schuster, Taftaf et al. 2021). CTC clusters may be more resistant to the form of apoptosis which results when cells lose their connections to other cells or to the cellular matrix, a phenomenon known as anoikis. Han et al. recently showed that fibronectin knockdown in breast and lung cancer cells caused a decrease in the expression of a variety of desmosomal proteins, including DSC2 and plakoglobin, culminating in reduced cellular aggregation and increased susceptibility to anoikis (Han, Sung et al. 2021).

The aforementioned mechanisms of enhanced cellular adhesion and CTC cluster formation indicate that, in terms of the metastasis cascade, DSC2 and PKP1 are foremost important in the dissemination phase of metastasis, enhancing the survival of the tumour cells in the circulation, rather than, for example, influencing the phases of proliferation, detachment, intravasation or extravasation.

2.6 Conclusions

The experimental data and results obtained from the analyses of clinical tumour tissue show that DSC2 and PKP1 may influence the progression and metastasis pattern of breast cancer. The results linked high DSC2 expression at an mRNA and protein level to the TNBC molecular subtype, a higher tumour grade and a significantly reduced disease-free survival. Tumours with increased DSC2 mRNA and/or protein expression were also more likely to metastasise to the brain and lungs. Increased PKP1 expression at an mRNA and protein level was associated with a higher incidence of locoregional and pulmonary metastases, as well as a reduced disease-free survival for breast cancer patients.

When considering the role of desmosomal proteins in maintaining intercellular contact, increased DSC2 and PKP1 expression may assist in the formation of tumour cell clusters, which are more robust and chemotherapy resistant, and thus more metastases prone than singular circulating tumour cells. Further insight into the intricacies of differential DSC2 and PKP1 expression and their specific influence on intercellular interactions may open new perspectives for DSC2 and PKP1 as diagnostic tools and as targets for therapeutic intervention. Future research could, for example, focus on the expression of these proteins specifically in CTC clusters and in other breast cancer metastatic entities, such as pulmonary metastases.

2.7 Abbreviations

TNBC	Triple negative breast cancer
HER2	Human epidermal growth factor receptor 2
CTCs	Circulating tumour cells
DSC2	Desmocollin 2
PKP1	Plakophilin 1
SDS	Sodium dodecyl sulphate
TBS(T)	Tris buffered saline (with tween)
TMA	Tissue microarray
ABC-HRP kit	Avidin-biotin enzyme complex - horseradish peroxidase kit
DAB	Diaminobenzidin
SPSS	Statistical Package for Social Sciences
ER	Oestrogen receptor
PR	Progesterone receptor
MCR	Multicellular resistance

3 Brief Summary of the Publication in English

This study investigated the role of the desmosomal protein DSC2 in the malignant progression of primary breast cancer cells and the formation of distant metastases. Firstly, the expression of DSC2 in primary breast cancer samples was quantified at a protein level using microarray and western blot analyses. These results, when analysed in conjunction with patient data, highlighted the prognostic value of DSC2, showing significantly higher DSC2 expression in the comparatively aggressive molecular subtypes HER2 and TNBC, when compared to luminal breast cancers. Furthermore, an increase in cerebral and lung metastases, as well as a reduction in disease-free and overall survival, was observed in cases with high DSC2 expression.

The direct influence of DSC2 expression on primary breast cancer cell behaviour and survival was subsequently investigated at a cellular level in both *in vitro* and *in vivo* experiments. Firstly, DSC2 overexpression and DSC2 knock down experiments were performed using the TNBC cell line MDA-MB-231 and the brain-seeking subline MDA-MB-231-BR. *In vitro* experiments on cell lines with DSC2 down regulation showed a significant decrease in cellular aggregation. Conversely, it could be shown that increased ectopic DSC2 expression resulted in increased cellular aggregation and improved chemoresistance in 3D structures. This influence could not be reproduced in 2D monolayered structures, further highlighting the importance of 3D cell aggregation for tumour cell drug resistance. The ensuing *in vivo* experiments using a brain dissemination xenograft mouse model underlined these findings, showing that DSC2 knock down in brain-seeking TNBC cells caused a significant reduction in both circulating tumour cells and tumour cell clusters, and, correspondingly, the formation of fewer and smaller brain metastases.

Our results suggest that DSC2 overexpression improves the metastatic capabilities of breast cancer cells by increasing tumour cell aggregation, thereby (1) enabling the formation of circulating tumour cell clusters - which are more resistant and prone to metastasise than single CTCs - and (2) hindering drug diffusion and protecting centrally located cells within both the primary tumour and in CTC clusters against drug exposition. Furthermore, we hypothesise that the increased DSC2 expression observed in the TNBC and HER2 subtypes is, at least in part, responsible for their comparatively higher metastatic potential and overall poorer prognosis.

4   Brief Summary of the Publication in German

Diese Studie untersuchte die Rolle des desmosomalen Proteins DSC2 bei der malignen Progression primärer Mammakarzinome und der Bildung von Fernmetastasen. Zunächst wurde die Expression von DSC2 in primären Mammakarzinomproben auf Proteinebene mithilfe von Microarray- und Western-Blot-Analysen quantifiziert. Diese Ergebnisse wurden mit Patientendaten statistisch korreliert und hoben einen prognostischen Wert von DSC2 hervor. Es zeigte sich eine deutlich höhere DSC2-Expression in den aggressiveren Subtypen HER2 und TNBC im Vergleich zum luminalen Mammakarzinom. Darüber hinaus wurde in Fällen mit hoher DSC2-Expression eine Zunahme von Hirn- und Lungenmetastasen sowie eine Verringerung des krankheitsfreien Überlebens und des Gesamtüberlebens beobachtet.

Der direkte Einfluss der DSC2-Expression auf das Verhalten und Überleben primärer Mammakarzinomzellen wurde anschließend auf zellulärer Ebene, sowohl in *In-vitro*- als auch *In-vivo*-Experimenten untersucht. Zunächst wurden DSC2-Überexpressions- und DSC2-Knockdown-Experimente mit der TNBC-Zelllinie MDA-MB-231 und der geneigt cerebral metastasierenden Zelllinie MDA-MB-231-BR durchgeführt. *In-vitro*-Experimente an Zelllinien mit DSC2-Knockdown zeigten eine signifikante Verminderung der Zellaggregation. Umgekehrt konnte gezeigt werden, dass eine erhöhte ektope DSC2-Expression zu einer erhöhten Zellaggregation und einer gesteigerten Chemoresistenz in 3D-Strukturen führte. Dieser Einfluss konnte in 2D-Monoschichtstrukturen nicht reproduziert werden, was die Bedeutung der 3D-Zellaggregaten für die Therapieresistenz von Tumorzellen weiter unterstreicht. Die anschließenden *In-vivo*-Experimente unter Verwendung eines gehirnmetastasierenden, xenotransplantatierten Mausmodells untermauerten diese Ergebnisse. Sie zeigten, dass eine reduzierte Expression von DSC2 in TNBC-Zellelinie MDA-MB-231R zu einer signifikanten Reduzierung sowohl der zirkulierenden Tumorzellen als auch der Tumorzellcluster und dementsprechend zur Bildung von weniger und kleineren Hirnmetastasen führte.

Unsere Ergebnisse legen nahe, dass die Überexpression von DSC2 die Metastasierungsfähigkeit zirkulierender Tumorzellen verbessert, indem sie indem sie die Tumorzellaggregation erhöht, wodurch (1) die Bildung zirkulierender Tumorzellcluster ermöglicht wird – die resistenter und anfälliger für Metastasierung sind als einzelne CTCs – und (2) Arzneimitteldiffusion behindert wird, und dadurch zentral gelegener Zellen vor Arzneimittelexposition geschützt werden. Zudem gehen wir davon aus, dass die erhöhte DSC2-Expression, die in den TNBC und HER2 Subtypen beobachtet wird, zumindest teilweise für deren vergleichsweise höheres Metastasierungspotenzial und die insgesamt schlechtere Prognose verantwortlich ist.

5   References

Aceto, N., A. Bardia, D. T. Miyamoto, M. C. Donaldson, B. S. Wittner, J. A. Spencer, M. Yu, A. Pely, A. Engstrom, H. Zhu, B. W. Brannigan, R. Kapur, S. L. Stott, T. Shioda, S. Ramaswamy, D. T. Ting, C. P. Lin, M. Toner, D. A. Haber and S. Maheswaran (2014). "Circulating tumor cell clusters are oligoclonal precursors of breast cancer metastasis." Cell **158**(5): 1110-1122.

Al-Jassar, C., H. Bikker, M. Overduin and M. Chidgey (2013). "Mechanistic basis of desmosome-targeted diseases." J Mol Biol **425**(21): 4006-4022.

Bartmann, C., M. Wischnewsky, T. Stuber, R. Stein, M. Krockenberger, S. Hausler, W. Janni, R. Kreienberg, M. Blettner, L. Schwentner, A. Wockel and J. Diessner (2017). "Pattern of metastatic spread and subcategories of breast cancer." Arch Gynecol Obstet **295**(1): 211-223.

Chang, P. H., M. C. Chen, Y. P. Tsai, G. Y. T. Tan, P. H. Hsu, Y. M. Jeng, Y. F. Tsai, M. H. Yang and W. W. Hwang-Verslues (2021). "Interplay between desmoglein2 and hypoxia controls metastasis in breast cancer." Proc Natl Acad Sci U S A **118**(3).

Desoize, B. and J. Jardillier (2000). "Multicellular resistance: a paradigm for clinical resistance?" Crit Rev Oncol Hematol **36**(2-3): 193-207.

Fang, W. K., L. D. Liao, L. Y. Li, Y. M. Xie, X. E. Xu, W. J. Zhao, J. Y. Wu, M. X. Zhu, Z. Y. Wu, Z. P. Du, B. L. Wu, D. Xie, M. Z. Guo, L. Y. Xu and E. M. Li (2013). "Down-regulated desmocollin-2 promotes cell aggressiveness through redistributing adherens junctions and activating beta-catenin signalling in oesophageal squamous cell carcinoma." J Pathol **231**(2): 257-270.

Fang, W. K., L. D. Liao, F. M. Zeng, P. X. Zhang, J. Y. Wu, J. Shen, L. Y. Xu and E. M. Li (2014). "Desmocollin-2 affects the adhesive strength and cytoskeletal arrangement in esophageal squamous cell carcinoma cells." Mol Med Rep **10**(5): 2358-2364.

Giuliano, M., A. Shaikh, H. C. Lo, G. Arpino, S. De Placido, X. H. Zhang, M. Cristofanilli, R. Schiff and M. V. Trivedi (2018). "Perspective on Circulating Tumor Cell Clusters: Why It Takes a Village to Metastasize." Cancer Res **78**(4): 845-852.

Haase, D., T. Cui, L. Yang, Y. Ma, H. Liu, B. Theis, I. Petersen and Y. Chen (2019). "Plakophilin 1 is methylated and has a tumor suppressive activity in human lung cancer." Exp Mol Pathol **108**: 73-79.

Han, H. J., J. Y. Sung, S. H. Kim, U. J. Yun, H. Kim, E. J. Jang, H. E. Yoo, E. K. Hong, S. H. Goh, A. Moon, J. S. Lee, S. K. Ye, J. Shim and Y. N. Kim (2021). "Fibronectin regulates anoikis resistance via cell aggregate formation." Cancer Lett **508**: 59-72.

Hegazy, M., A. L. Perl, S. A. Svoboda and K. J. Green (2022). "Desmosomal Cadherins in Health and Disease." Annu Rev Pathol **17**: 47-72.

Hou, J. M., M. G. Krebs, L. Lancashire, R. Sloane, A. Backen, R. K. Swain, L. J. Priest, A. Greystoke, C. Zhou, K. Morris, T. Ward, F. H. Blackhall and C. Dive (2012). "Clinical significance and molecular characteristics of circulating tumor cells and circulating tumor microemboli in patients with small-cell lung cancer." J Clin Oncol **30**(5): 525-532.

Klotz, R., A. Thomas, T. Teng, S. M. Han, O. Iriondo, L. Li, S. Restrepo-Vassalli, A. Wang, N. Izadian, M. MacKay, B. S. Moon, K. J. Liu, S. K. Ganesan, G. Lee, D. S. Kang, C. S. Walmsley, C. Pinto, M. F. Press, W. Lu, J. Lu, D. Juric, A. Bardia, J. Hicks, B. Salhia, F. Attenello, A. D. Smith and M. Yu (2020). "Circulating Tumor Cells Exhibit Metastatic Tropism and Reveal Brain Metastasis Drivers." Cancer Discov **10**(1): 86-103.

Landemaine, T., A. Jackson, A. Bellahcene, N. Rucci, S. Sin, B. M. Abad, A. Sierra, A. Boudinet, J. M. Guinebretiere, E. Ricevuto, C. Nogues, M. Briffod, I. Bieche, P. Cherel, T. Garcia, V. Castronovo, A. Teti, R. Lidereau and K. Driouch (2008). "A six-gene signature predicting breast cancer lung metastasis." Cancer Res **68**(15): 6092-6099.

Li, K., R. Wu, M. Zhou, H. Tong and K. Q. Luo (2021). "Desmosomal proteins of DSC2 and PKP1 promote cancer cells survival and metastasis by increasing cluster formation in circulatory system." Sci Adv **7**(40): eabg7265.

Liang, Y., H. Zhang, X. Song and Q. Yang (2020). "Metastatic heterogeneity of breast cancer: Molecular mechanism and potential therapeutic targets." Semin Cancer Biol **60**: 14-27.

Marrella, A., A. Fedi, G. Varani, I. Vaccari, M. Fato, G. Firpo, P. Guida, N. Aceto and S. Scaglione (2021). "High blood flow shear stress values are associated with circulating tumor cells cluster disaggregation in a multi-channel microfluidic device." PLoS One **16**(1): e0245536.

Martin-Padron, J., L. Boyero, M. I. Rodriguez, A. Andrades, I. Diaz-Cano, P. Peinado, C. Balinas-Gavira, J. C. Alvarez-Perez, I. F. Coira, M. E. Farez-Vidal and P. P. Medina (2020). "Correction: Plakophilin 1 enhances MYC translation, promoting squamous cell lung cancer." Oncogene **39**(32): 5494.

Saias, L., A. Gomes, M. Cazales, B. Ducommun and V. Lobjois (2015). "Cell-Cell Adhesion and Cytoskeleton Tension Oppose Each Other in Regulating Tumor Cell Aggregation." Cancer Res **75**(12): 2426-2433.

Schnitt, S. J. (2010). "Classification and prognosis of invasive breast cancer: from morphology to molecular taxonomy." Mod Pathol **23 Suppl 2**: S60-64.

Schuster, E., R. Taftaf, C. Reduzzi, M. K. Albert, I. Romero-Calvo and H. Liu (2021). "Better together: circulating tumor cell clustering in metastatic cancer." Trends Cancer **7**(11): 1020-1032.

Smid, M., Y. Wang, Y. Zhang, A. M. Sieuwerts, J. Yu, J. G. Klijn, J. A. Foekens and J. W. Martens (2008). "Subtypes of breast cancer show preferential site of relapse." Cancer Res **68**(9): 3108-3114.

Soni, A., Z. Ren, O. Hameed, D. Chanda, C. J. Morgan, G. P. Siegal and S. Wei (2015). "Breast cancer subtypes predispose the site of distant metastases." Am J Clin Pathol **143**(4): 471-478.

South, A. P. (2004). "Plakophilin 1: an important stabilizer of desmosomes." Clin Exp Dermatol **29**(2): 161-167.

Sung, H., J. Ferlay, R. L. Siegel, M. Laversanne, I. Soerjomataram, A. Jemal and F. Bray (2021). "Global Cancer Statistics 2020: GLOBOCAN Estimates of Incidence and Mortality Worldwide for 36 Cancers in 185 Countries." CA Cancer J Clin **71**(3): 209-249.

Ward, J. M. and J. E. Rehg (2014). "Rodent immunohistochemistry: pitfalls and troubleshooting." Vet Pathol **51**(1): 88-101.

Winters, S., C. Martin, D. Murphy and N. K. Shokar (2017). "Breast Cancer Epidemiology, Prevention, and Screening." Prog Mol Biol Transl Sci **151**: 1-32.

Xie, N., Z. Hu, C. Tian, H. Xiao, L. Liu, X. Yang, J. Li, H. Wu, J. Lu, J. Gao, X. Hu, M. Cao, Z. Shui and Q. Ouyang (2020). "In Vivo Detection of CTC and CTC Plakoglobin Status Helps Predict Prognosis in Patients with Metastatic Breast Cancer." Pathol Oncol Res **26**(4): 2435-2442.

Yang, C., R. Fischer-Keso, T. Schlechter, P. Strobel, A. Marx and I. Hofmann (2015). "Plakophilin 1-deficient cells upregulate SPOCK1: implications for prostate cancer progression." Tumour Biol **36**(12): 9567-9577.

6 Declaration of Author's Own Contribution

The foundation of this study evolved from the work of Prof. Dr. Leticia Oliveira-Ferrer, who performed the original microarray analyses on primary breast cancer tissue samples and, on the basis of these results, hypothesised an association between increased DSC2 and PKP1 expression and the development of cerebral metastases.

Prof. Dr. Leticia Oliveira-Ferrer designed and supervised the ensuing experiments at a protein level. Kathrin Eylmann prepared the western blot protein lysates from fresh frozen tissue samples obtained intraoperatively from primary breast cancer patients. I was personally responsible for performing, quantifying, and evaluating the results of all western blot experiments. I personally performed all statistical analyses using SPSS Statistics and was responsible for the graphical presentation of my results.

With the assistance of Prof. Dr. Leticia Oliveira-Ferrer and Kathrin Eylmann, I established and optimised new immunohistochemistry protocols for DSC2 and PKP1. The two-person interpretation of the slide staining was performed by myself and Prof. Dr. Leticia Oliveira-Ferrer. I was responsible for the digital presentation of these results, which were not included in the final draft of the publication.

Subsequent to my experiments and on the basis of my results, further *in vitro* and *in vivo* experiments were performed by the other contributing authors. As such, the resulting publication was a collaboration between all contributing authors. As the only author with English as a first language, I contributed significantly to the written text of the manuscript and in the proof-reading phase of publication.

7 Acknowledgements

8 Curriculum Vitae

<u>**PERSÖNLICHE ANGABEN**</u>

Name:	Sarah Giannini Bryan
Geburtsdatum:	09.12.1991
Geburtsort:	Carlton, Melbourne, Australien
Nationalitäten:	australisch und italienisch
Familienstand:	verheiratet

<u>**BILDUNGSWEG**</u>

10/2014- 05/2021	Studium der Humanmedizin, Universitätsklinikum Hamburg Eppendorf (UKE)
	• Approbation 06/2021
03/2011- 1/2013	Bachelor of Science, Universität Melbourne
	• Anatomie, Physiologie, Biochemie, Neurowissenschaften, Genetik und Mikrobiologie
	• Freemover Semester, Molecular Life Sciences, Universität Hamburg (2013)
2009	Abitur, Box Hill High School, Melbourne

<u>**KLINISCHE ARBEIT**</u>

06/2021 - heute	Assistenzärztin in Weiterbildung
	• Abteilung für Gynäkologie und Geburtshilfe, Albertinen Krankenhaus, Hamburg
05/2020 - 04/2021	Praktisches Jahr
	• Allgemeinchirurgie, Schön Klinik Eilbek
	• Allgemein-, Gefäßchirurgie und Orthopädie, Bürgerspital Solothurn, Schweiz
	• Gynäkologie und Geburtshilfe, Albertinen Krankenhaus
	• Innere Medizin, Schön Klinik Eilbek
03/2016 - 05/2021	Studentische Aushilfskraft, UKE

<u>**WISSENSCHAFTLICHE ARBEIT UND PUBLIKATIONEN**</u>

03/2017 - heute	Angestrebte Publikationspromotion
	• Reimer F, Bryan S et al. The role of the desmosomal protein desmocollin 2 in tumour progression in triple negative breast cancer patients. Cancer Cell Int. 2023 Mar 16
08/2021	Publikation (Review)
	• Bryan S et al. Molecular Mechanisms Associated with Brain Metastases in HER2-Positive and Triple Negative Breast Cancers. Cancers (Basel). 2021 Aug 17
04/2019 - 05/2021	Leiterin des "English journal clubs" für Pflegewissenschaften, UKE
10/2017	Poster-Präsentation
	• auf dem 8. wissenschaftlichen Symposium der Kommission Translationaler Forschung (TRAFO) der Arbeitsgemeinschaft Gynäkologische Onkologie, Düsseldorf
03/2017 - 10/2017	Experimentelle Laborarbeiten, Gynäkologisches Forschungslabor, UKE
	• Doktormutter: Prof. Dr. Leticia Oliveira-Ferrer

<u>**STIPENDIEN UND AUSZEICHNUNGEN**</u>

2019 - 2021	Stipendiatin des Deutschlandstipendiums
2020	Hamburg Global Förderung
2018	Reisestipendium für den 62. DGGG-Kongress, Berlin
2017	Studienbeihilfe der Rolfing-Stiftung
2017	Reisestipendium für das TraFo Symposium 2017, Düsseldorf
2012	Melbourne Global Language Stipendium

9   Statutory declaration/ Eidesstattliche Versicherung

Ich versichere ausdrücklich, dass ich die Arbeit selbständig und ohne fremde Hilfe verfasst, andere als die von mir angegebenen Quellen und Hilfsmittel nicht benutzt und die aus den benutzten Werken wörtlich oder inhaltlich entnommenen Stellen einzeln nach Ausgabe (Auflage und Jahr des Erscheinens), Band und Seite des benutzten Werkes kenntlich gemacht habe.

Ferner versichere ich, dass ich die Dissertation bisher nicht einem Fachvertreter an einer anderen Hochschule zur Überprüfung vorgelegt oder mich anderweitig um Zulassung zur Promotion beworben habe.

Ich erkläre mich einverstanden, dass meine Dissertation vom Dekanat der Medizinischen Fakultät mit einer gängigen Software zur Erkennung von Plagiaten überprüft werden kann.

Unterschrift: ....